Recent Advances in Global Wave Activity Analysis from Long-Term GPS RO Data

A. de la Torre (1), P. Alexander (1), P. Llamedo (1)
T. Schmidt (2), and J. Wickert (2)

(1) Departamento de Fisica, FCEN, Universidad de Buenos Aires, Argentina
(2) GeoForschungsZentrum (GFZ) Potsdam, Potsdam, Germany

Topics:

- Long-term global atmospheric wave activity analysis and observations in the lower and middle atmosphere from a long term period of GPS RO observations with CHAMP, SAC-C and GRACE LEOs.

- Monthly, seasonal, interannual and quasibiennial variability with latitude, longitude and altitude.

- Possible limitations and distortions imposed by the relative geometry of wave phase surfaces, lines of sight and of tangent points during each occultation. Possible calculation of potential energy and mean potential energy from temperature, potential temperature or refractivity, choosing different averaging criteria and band-pass filtering cutoffs.

- Detection of two high WA events from the global analysis. Numerical simulation of these events to study their origin and characteristics. Discussion of discrepancies between RO and mesoscale simulations.

- J. Alexander (1998): No observational technique is able by itself to contemplate the whole spectrum of GWs
- Tsuda et al (2000) (GPS MET): Latitude, longitude, altitude and seasonal variability in the stratosphere
- Venkat Ratnam et al (2004) (CHAMP): Large/low values of WA below/above 25 km, increasing again above 30 km and during stratospheric warming of Sep 2002
- Randel and Wu (2005): KW variability during two years
- Smith et al (2006): Multiple tropopauses from CHAMP
- Baumgaertnet and McDonald (2007): GWs over Antartica from CHAMP

- Mean specific (per unit mass) potential energy associated with a single monochromatic wave of vertical wavelength λ_z is
  $EP_{\lambda z} = \lambda_z^{-1} \int_0^{\lambda_z} EPdz$

- $EP = g^2 \delta T^2 / 2N^2 T^2_B$: Specific potential energy

- T(z) profiles were splined with a 200 m step

- Band-passed δT fluctuations are between cut-offs z_1 and z_2. T(z) profiles were first low pass filtered, with a cut-off at z_2, obtaining T_B

- The filter was applied again to the difference $T - T_B$, now with a cut-off at z_1, thus yielding δT, thus isolating vertical wavelengths between z_1 and z_2

- Two different non-recursive filters were tested [Scavuzzo et al, 1988; Schönwiese, 2000], with almost identical results.

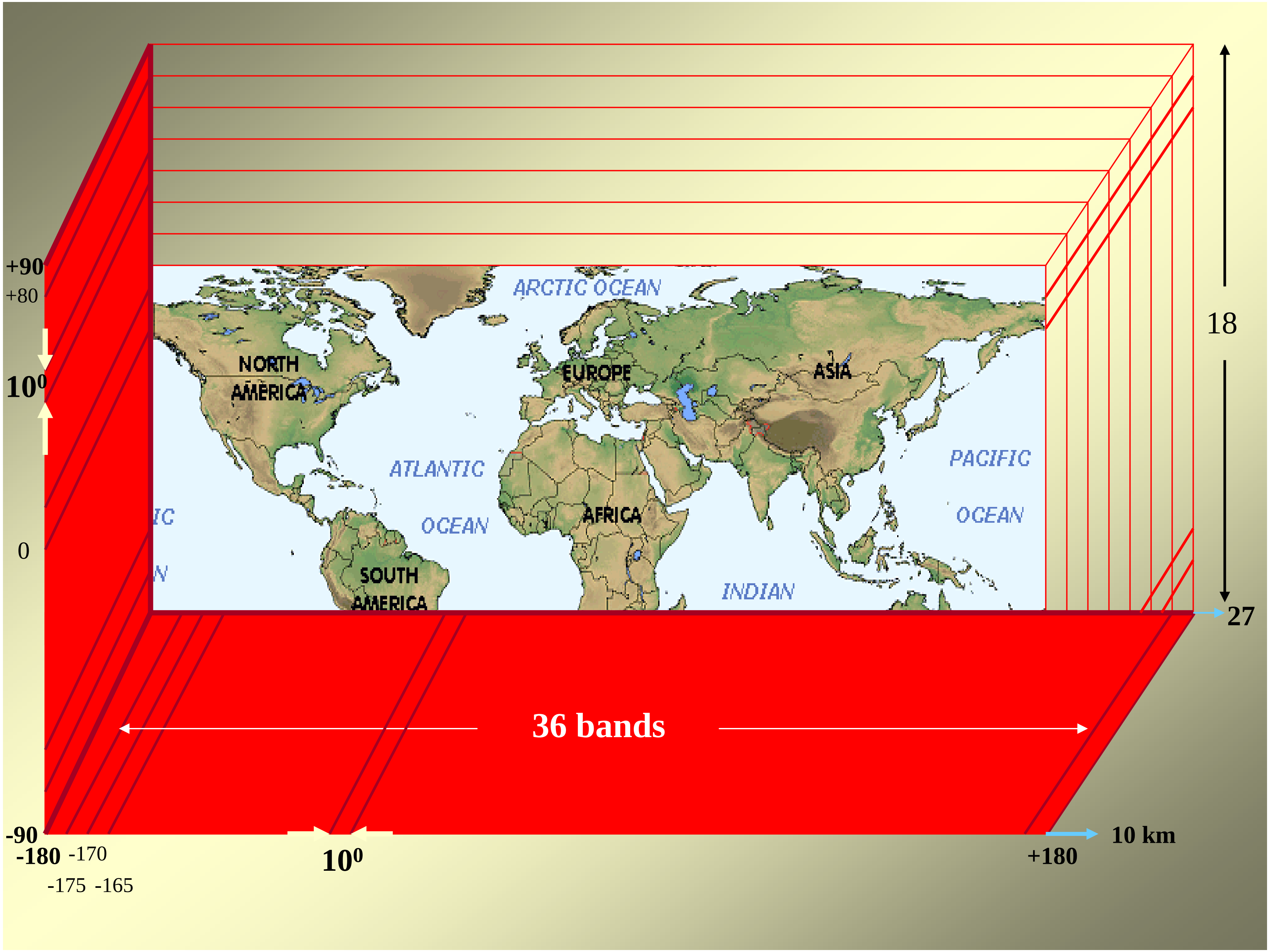

+90
+80
10^0
0
-90
-180
-170
-175
-165
10^0
36 bands
+180
10 km
27
18
ARCTIC OCEAN
NORTH AMERICA
EUROPE
ASIA
ATLANTIC
OCEAN
AFRICA
PACIFIC
OCEAN
SOUTH AMERICA
INDIAN

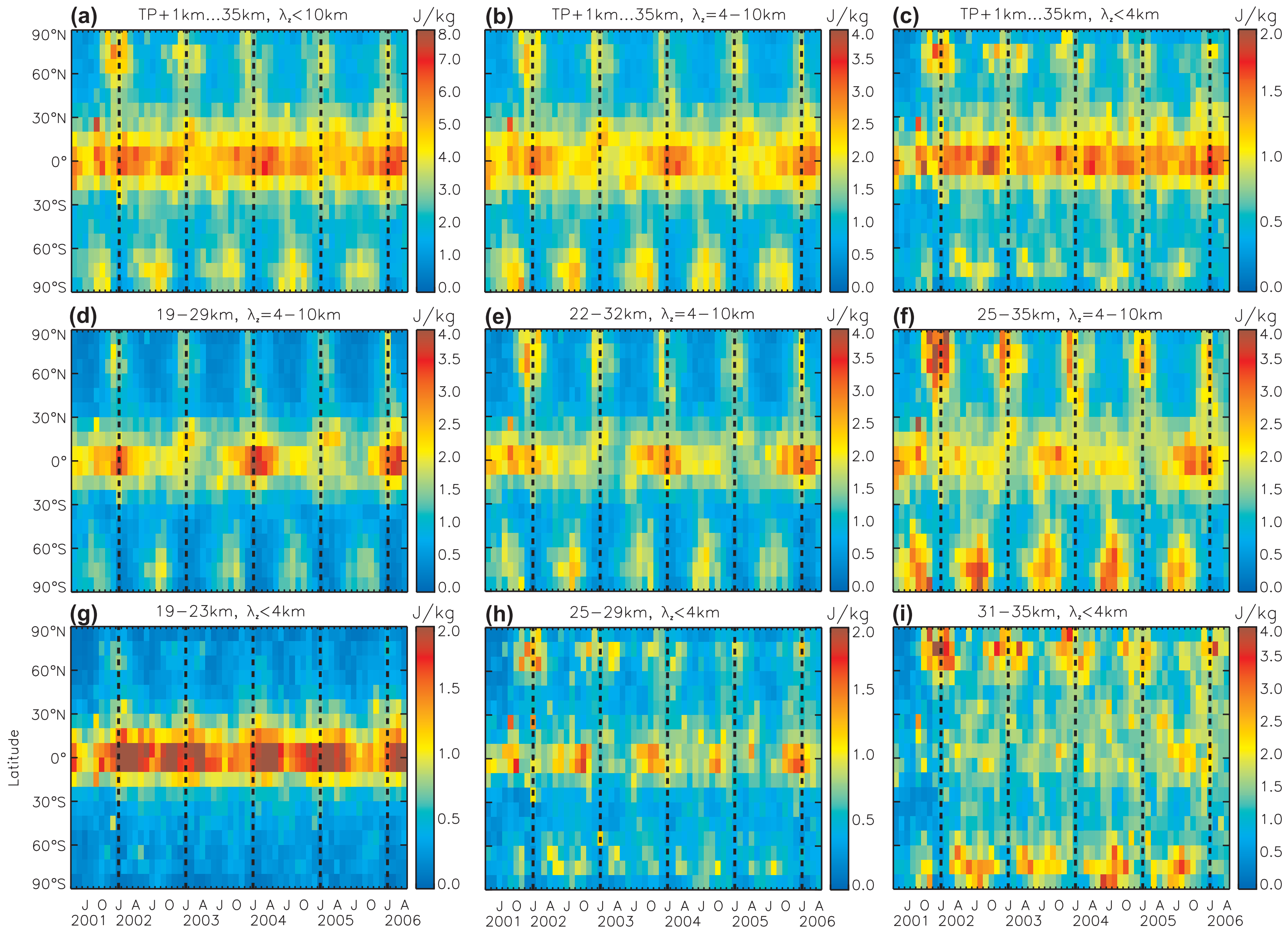

For short λ_z, an equatorial annual enhanced WA is only observed within 19-23 km between +/-20^0 and to a lesser extent, within 25-29 km. There is a weakening of this periodic behavior around the equator and a progressive enhancement of extratropical high latitude WA with increasing z .
At 31-35 km maximum E_{PC} values are found only at high latitudes.

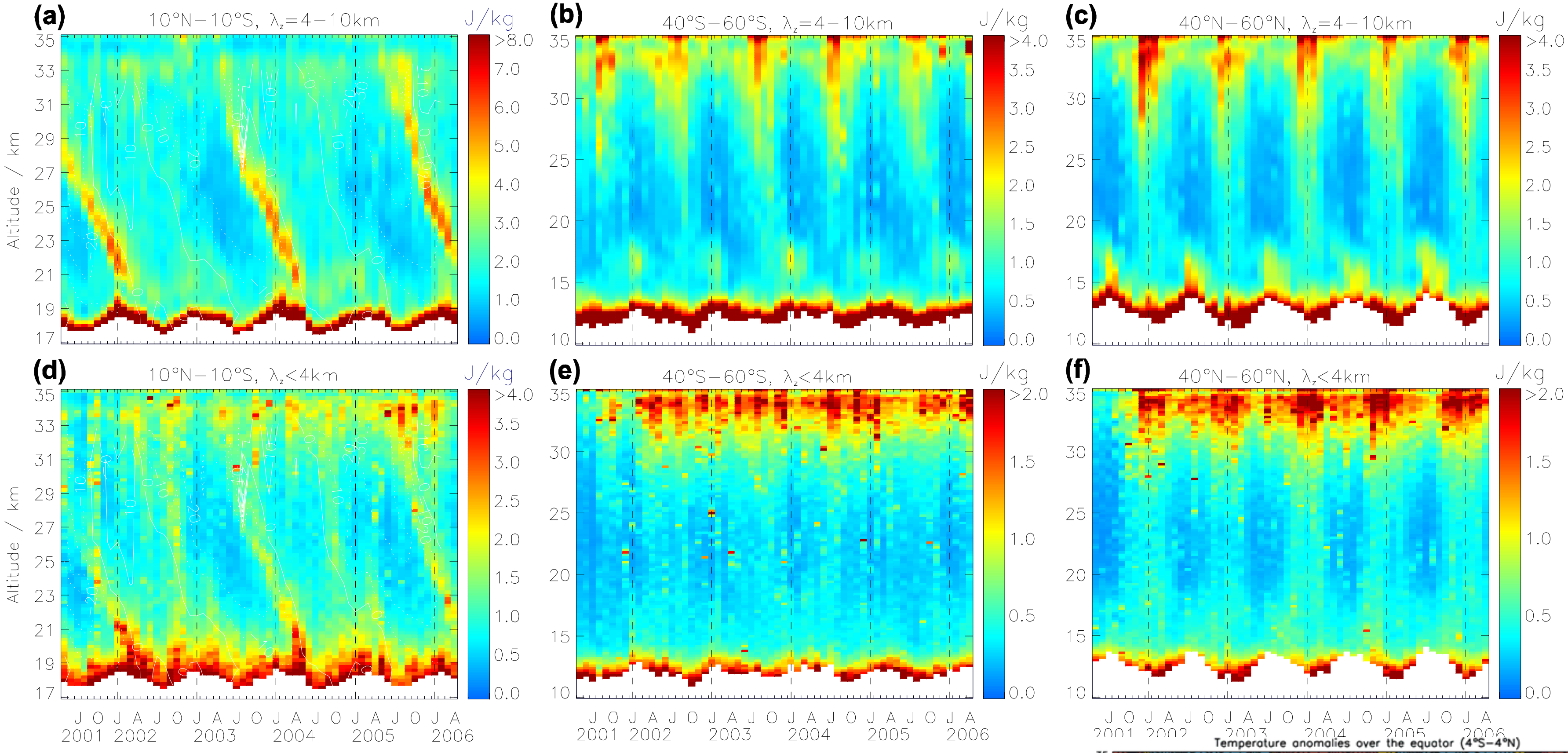

For short vertical wavelengths, the WA distribution in d) is similar to a), but reaching only half the maximum E_P values. Finally, in e) and f) we only remark a persistent WA near to the TP and from 25 to 35 km (mainly in winter NH).

- A part of the wave spectrum was rejected by filtering out scales longer than 10 km
- It is not possible to fully resolve GWs from RO measurements because there are different kinds of distortions. A discrepancy is expected between "actual" and "apparent" λ_z, due to the non-vertical line of tangent points (LTP) followed during the atmospheric soundings, in a scenario of phase surfaces distributed over a wide range of wave propagation bending angles
- The wavelength refraction in a ground-fixed frame of reference imposed by a variable background mean wind

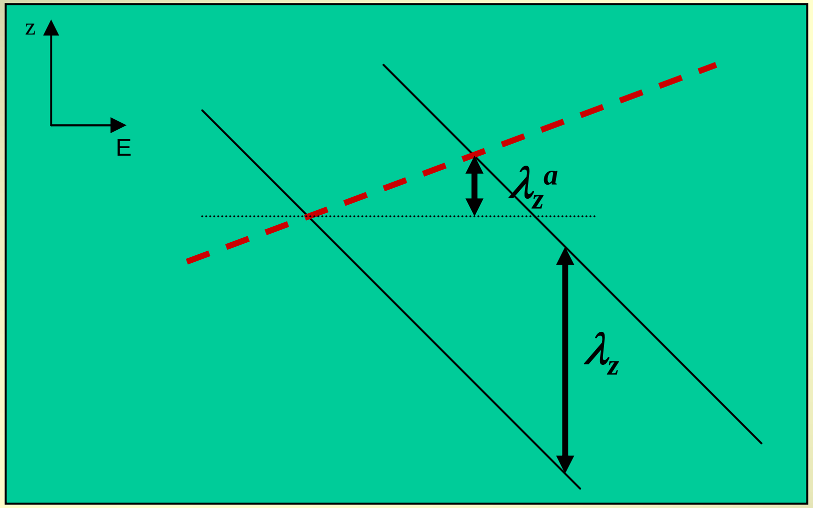

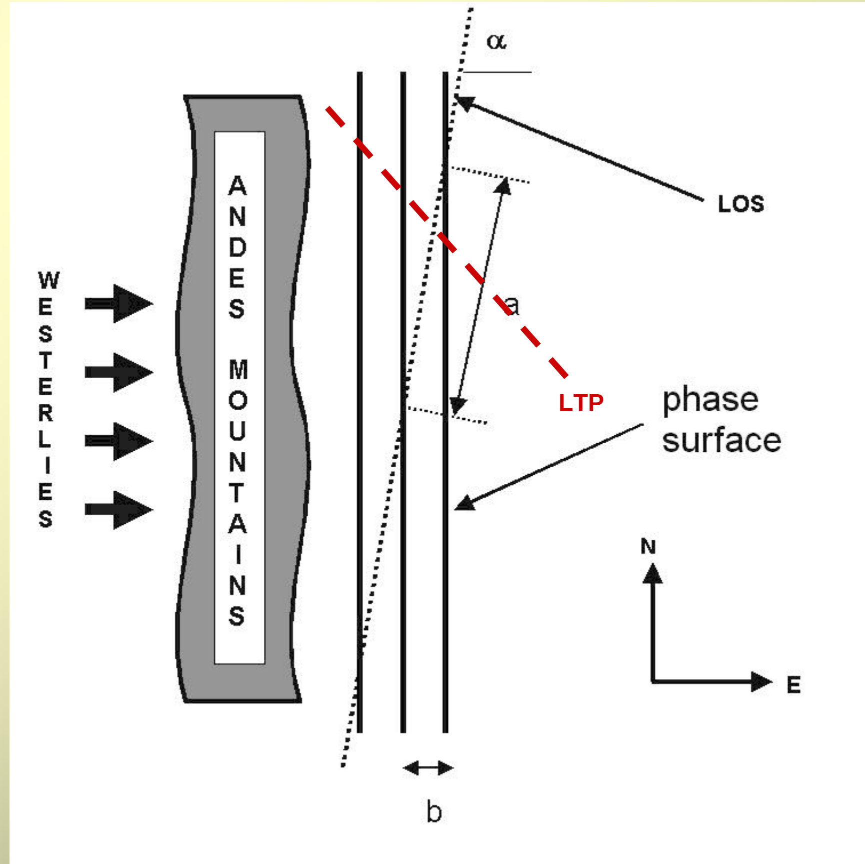

- The uncertain capability of RO measurements to detect short horizontal wavelengths, considering the relative direction between lines of sight (LOS) and lines of tangent points (LTP) both respect to GW phase front surfaces. The outcome in each occultation depends on the characteristics of the waves (essentially the wavelengths and amplitudes)

- These distortions may derive in possible over or underestimations of EP and consequently, of $EP_{\lambda z}$

- Ideal conditions for faith wave amplitude in occultation retrievals are given by quasi horizontal wave phase surfaces or when the LOS and LTP are respectively nearly contained and out of those planes. Short horizontal scale waves are filtered out with high probability (but not certainly, due to the "magnifying" effect on the observed horizontal wavelength when the angle between the line of sight and the horizontal wave vector approaches 90 deg. Extreme caution is needed when addressing the issues of amplitude, wavelength and phase of gravity waves in occultation data.

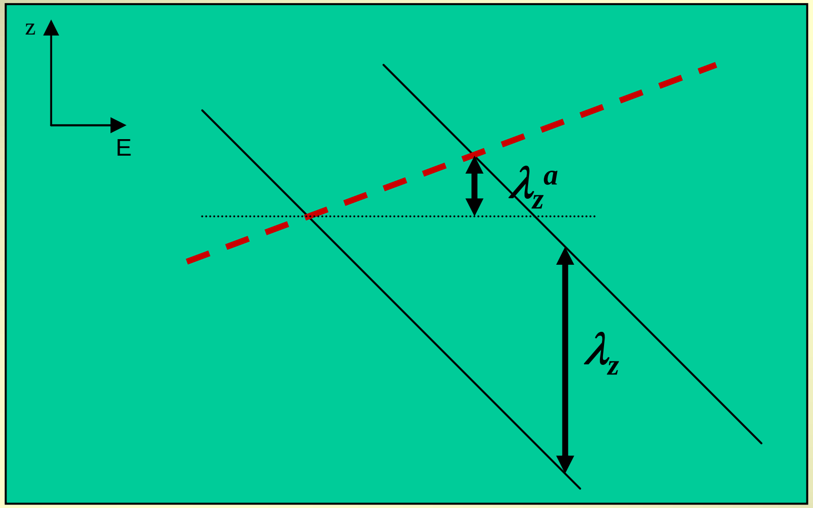

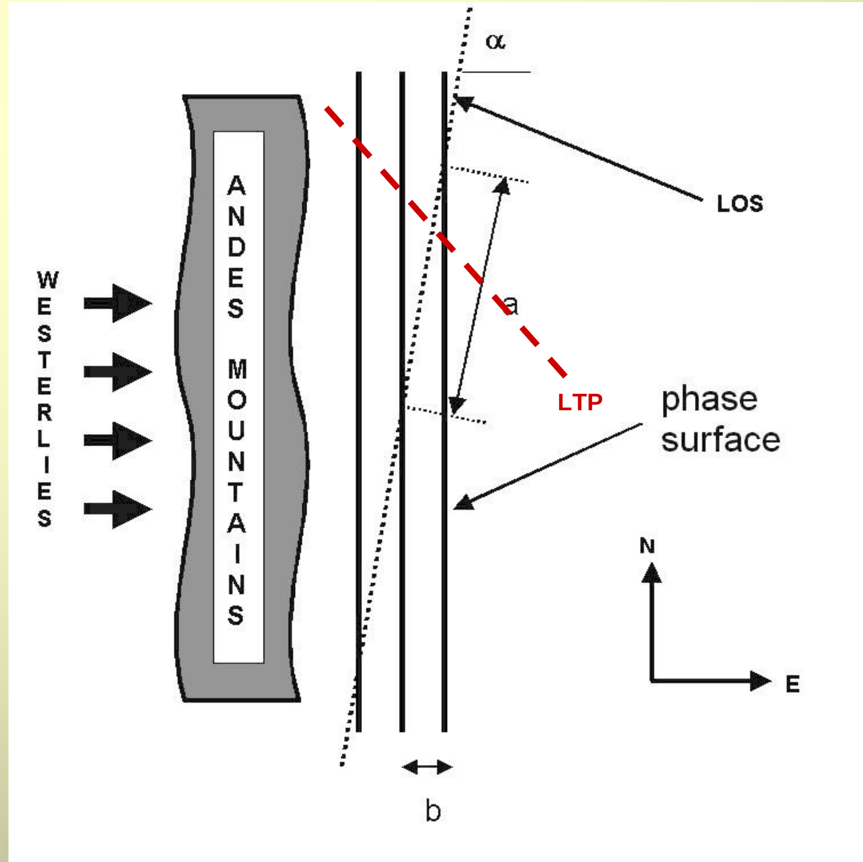

- In order to get insight into the quantitative significance of the retrieved temperature perturbations, from our global analysis now monthly averaged in latitude-longitude plots,

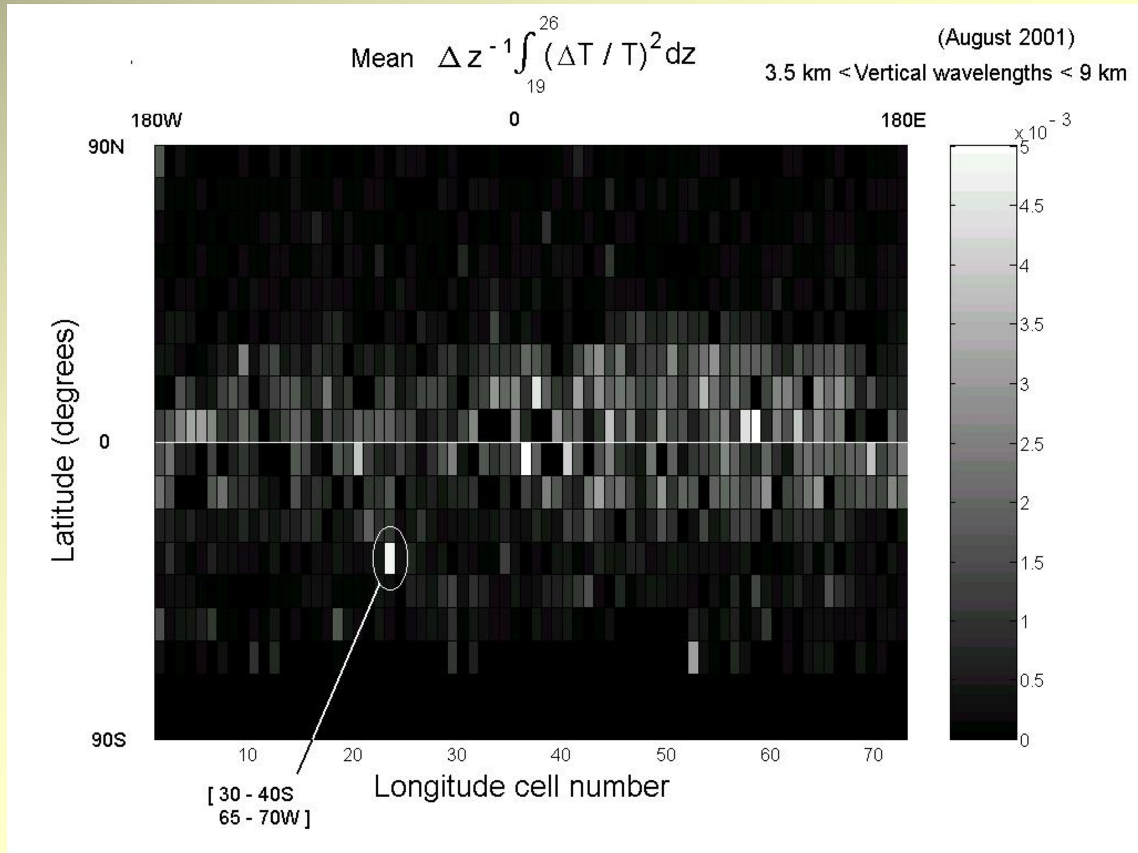

we selected two intense RO events:

1. 30 Aug 2001, 04:10 UTC and
2. 20 Nov 2001, 03:58 UTC (in what follows, S1 and S2 respectively)

- Both cases were detected near to Andes mountains, were usually large amplitude mountain waves are observed during stable conditions. These waves may be enhanced in the presence of jets, avoiding critical level filtering. We remark here that the region constitutes a natural laboratory were the three main GW sources are expected to coexist: mountain forcing, geostrophic adjustment and convective generation.

- In the figure, the topography and horizontal projections of LOS and LTP are indicated. Observe that LTP corresponding to S1 is situated over the mountains, whereas in the case of S2 it is situated approximately at 200km east of the mountain over a plateau region.

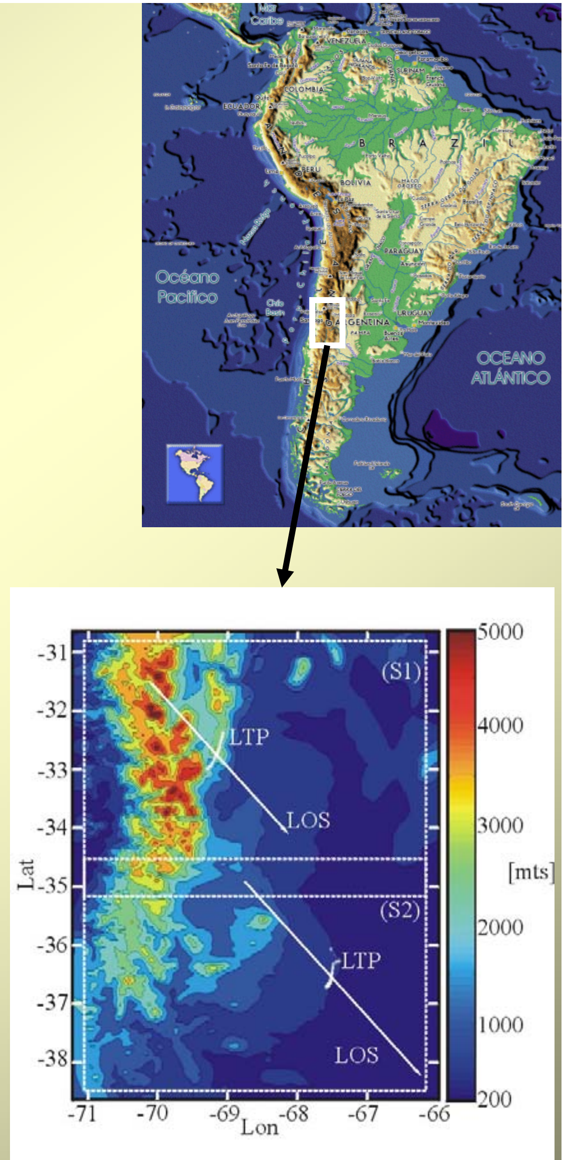

- We performed simulations using MM5 and WRF mesoscale models during both events, obtaining identical results. Our objective here was to understand the origin and characteristics of the perturbations detected during both RO events.

- In both cases we employed three nested domains with effective horizontal grid spacing of 36 km (see external domain for both simulations in the figure), 12 km, and 4 km respectively. The experiments were driven by assimilating lateral boundary conditions and sea surface temperatures from NCEP reanalysis. Both simulations were initialized at least one day before the respective RO events in order to stabilize them.

(The following main physical parameterizations were employed: Kain-Fritsch (1993) cumulus convection, explicit moisture scheme including simple ice physics (Dudhia, 1989), cloud-radiation (Benjamin and Carlson, 1986) and NCEP Medium-Range Forecast Model planetary boundary layer).

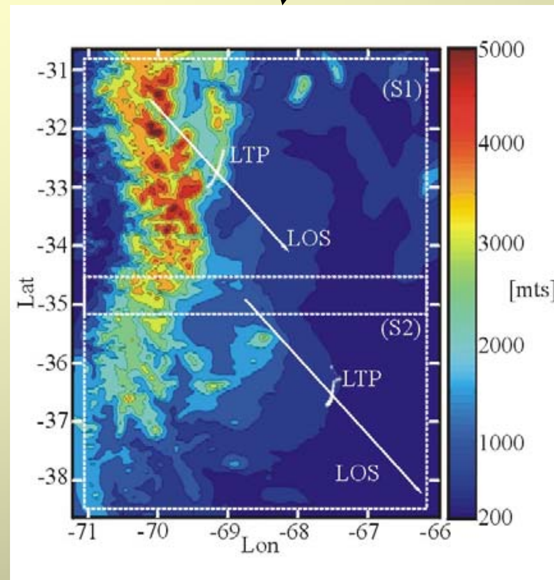

The simulations exhibit good performance and reproduce various characteristics of southern South America regional climatology [Menéndez et al,2004]:

1. Typical westerlies at and above 700mb during both events.

2. An intense jet core with zonal speed > 50m/sec at 250mb.

3. A jet core intensity varying more rapidly than the inertial period. Probable IGWs radiated by geostrophic adjustment must be considered.

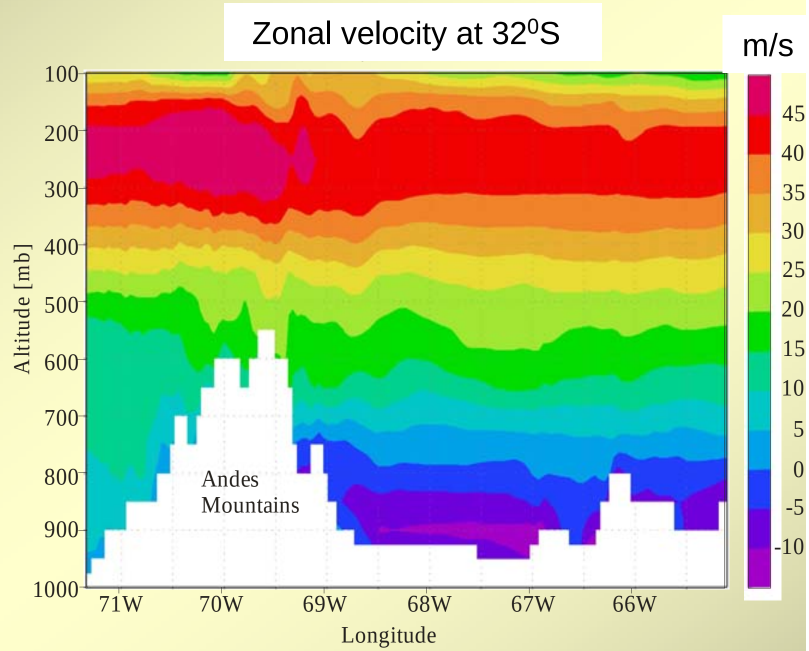

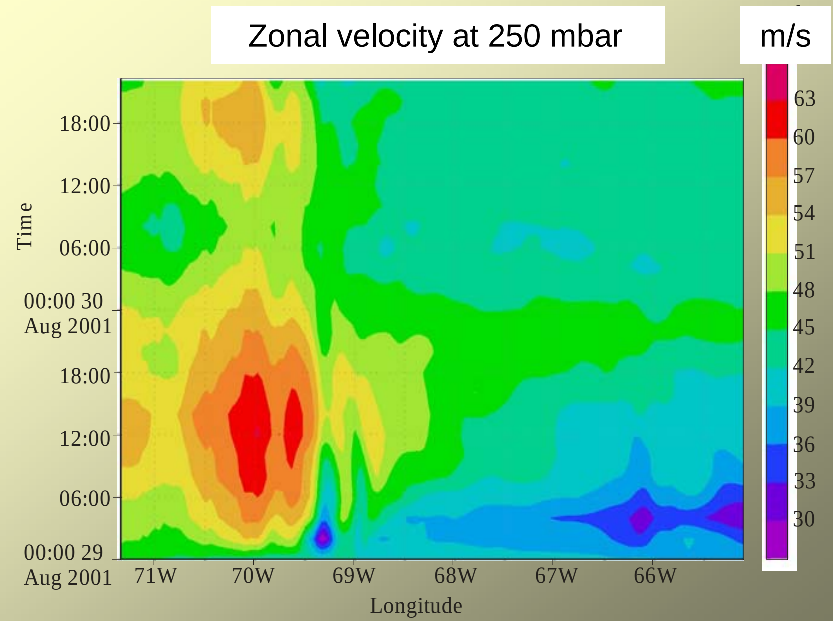

The generation of IGWs by geostrophic adjustment near the permanent jets above the Andes Mountains at midlatitudes (30-40S) must be also considered, when the timescale of evolution of the background becomes comparable or shorter than the inertial period.

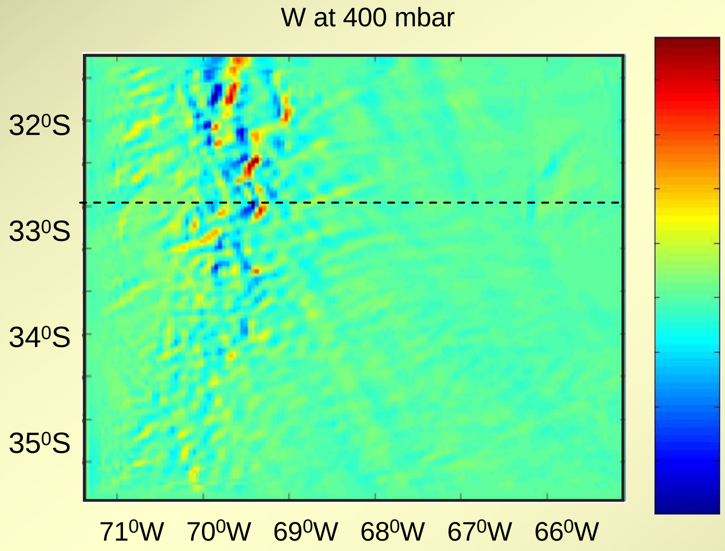

Downward/upward phase propagations above/below jets are usually seen [Hirota and Niki,1985; Thomas et. a.,1992]. In the region here studied, MWs in the vicinity of a jet stream, may provide the necessary body forcing and constitute an almost permanent perturbation to a geostrophic balanced flow, thus giving rise to IGWs.

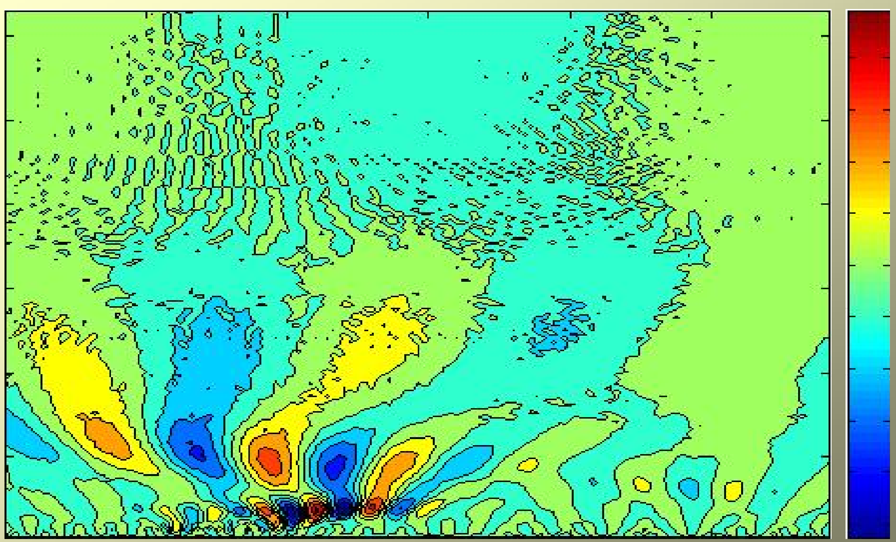

In the hodograph it can be seen that the velocity vector rotates counter-clockwise toward East, even at 400mb (below the jet), evidencing together with phase surface slopes a downward phase velocity.

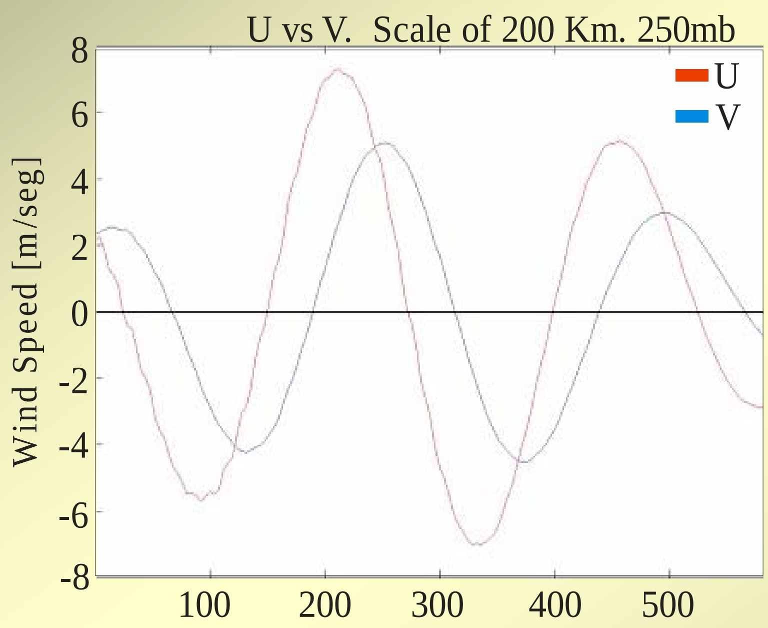

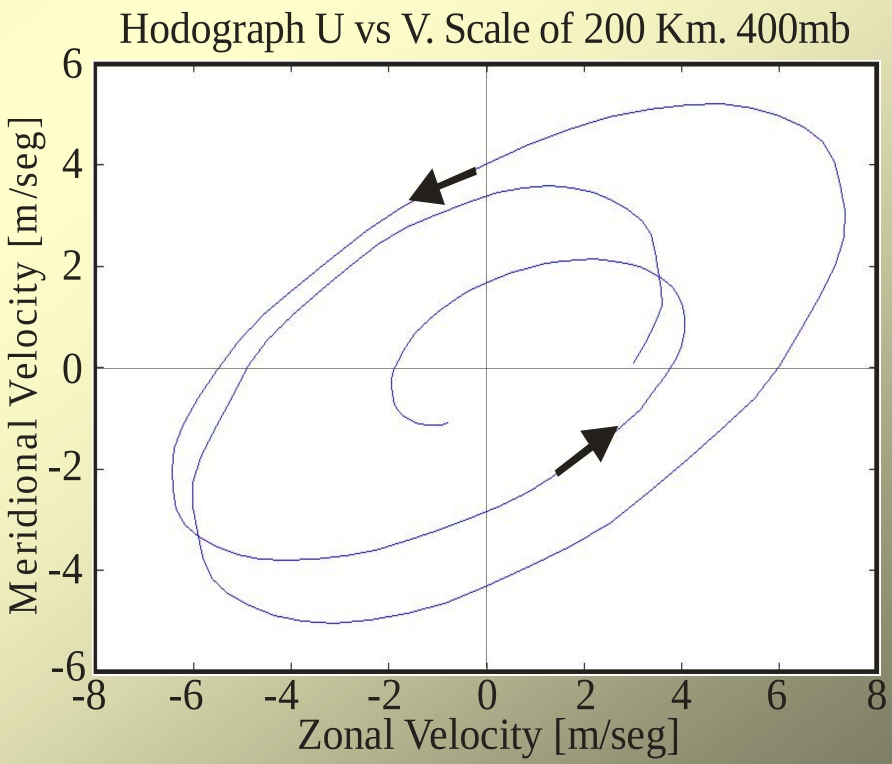

Now that we conclude that the wave perturbations detected from RO and WRF are due to mountain forcing, we plot below T as retrieved at RO tangent points and from WRF constant pressure levels, for both events

As expected, WRF shows:

1. For S1, a considerable wave variability near to the mountains, and
2. For S2, a poor WA far from the mountains

The question here is: Why do we detect, nevertheless, high WA in both events in our global GW climatology?

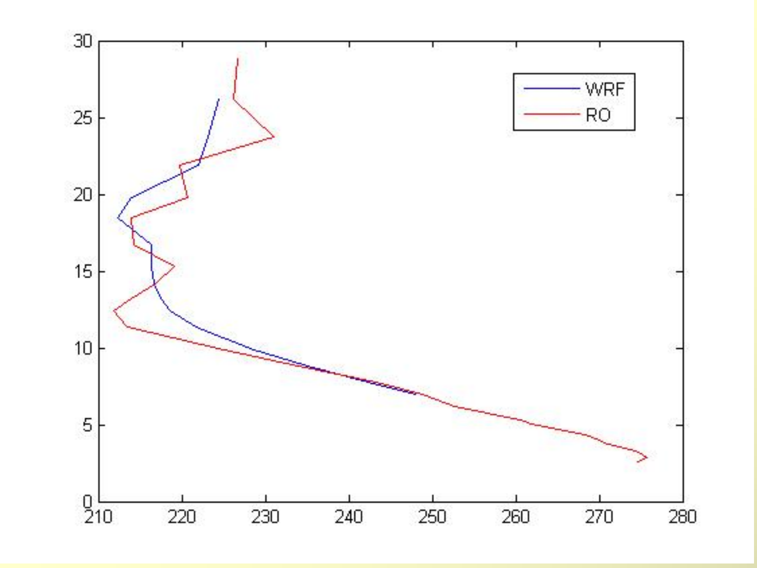

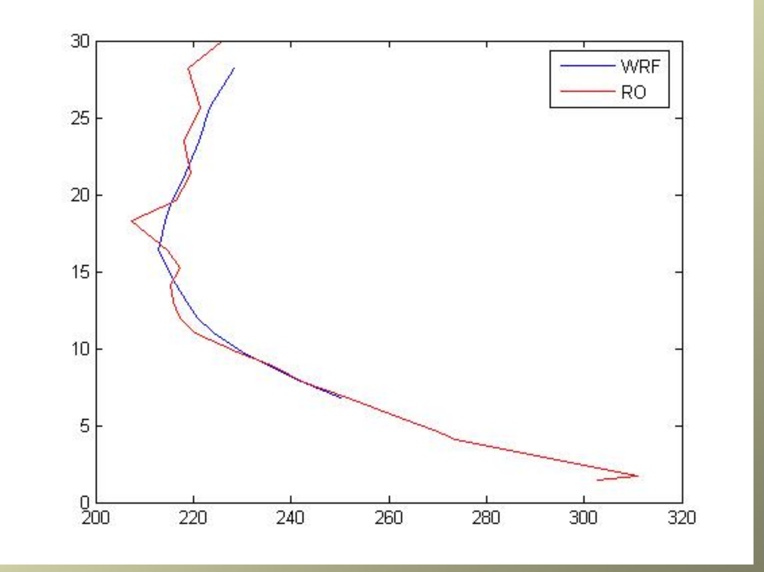

- **In case S1**, both LTP and LOS fall well inside an atmospheric region with high WA:

WRF Simulation 04:00 UTC 30AUG 2001

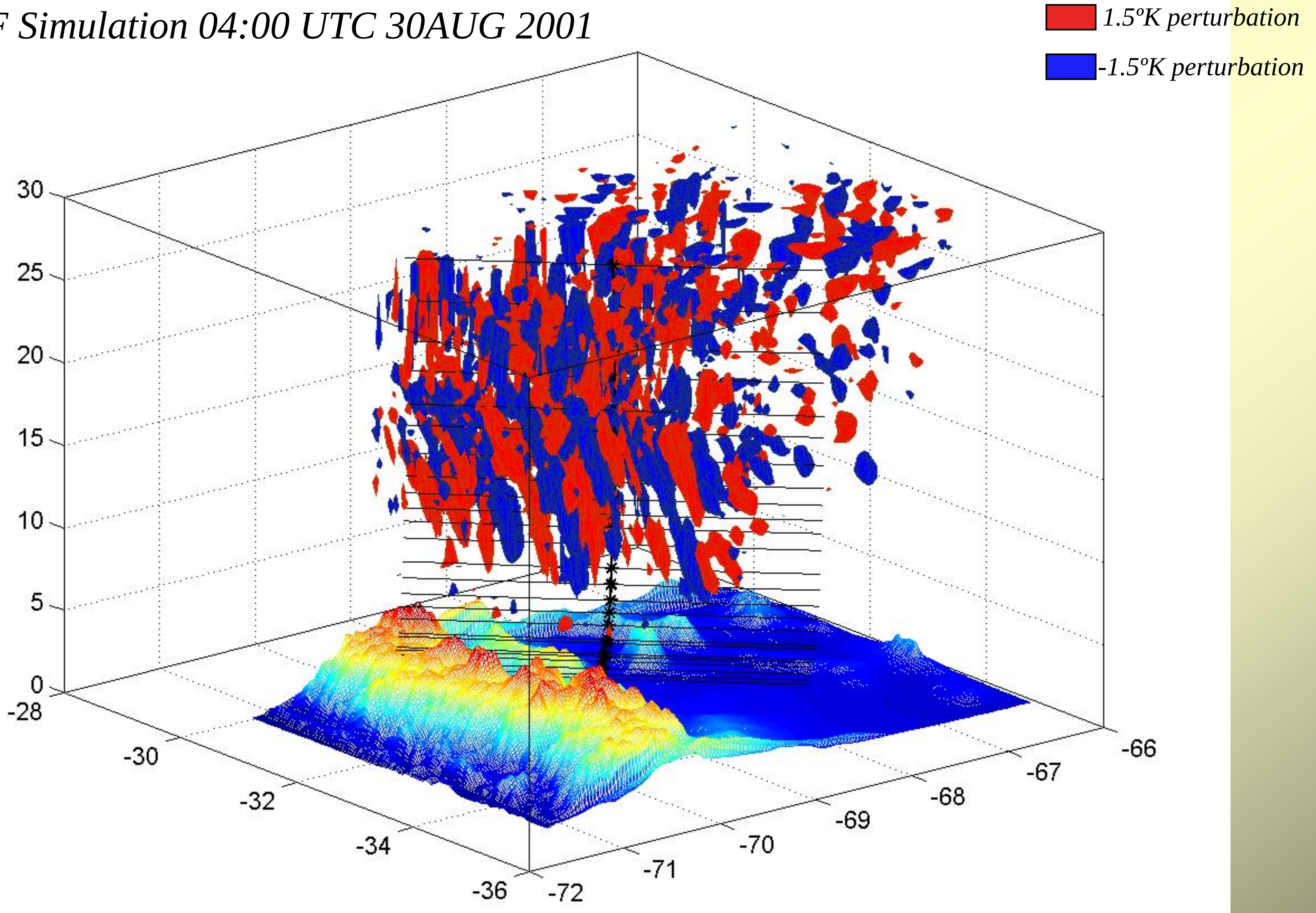

WRF Simulation 04:00 UTC 30AUG 2001

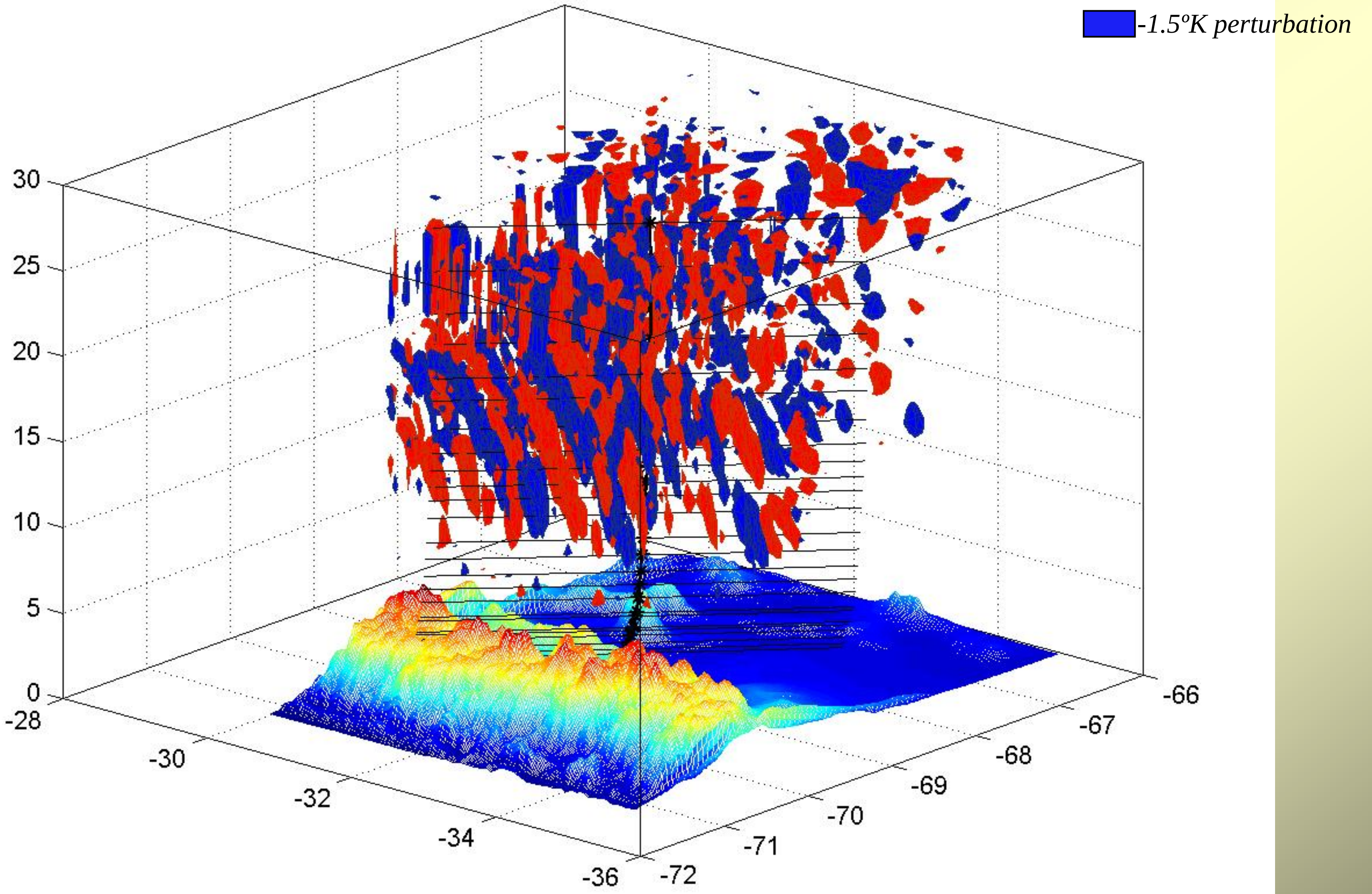

WRF Simulation 04:00 UTC 30AUG 2001

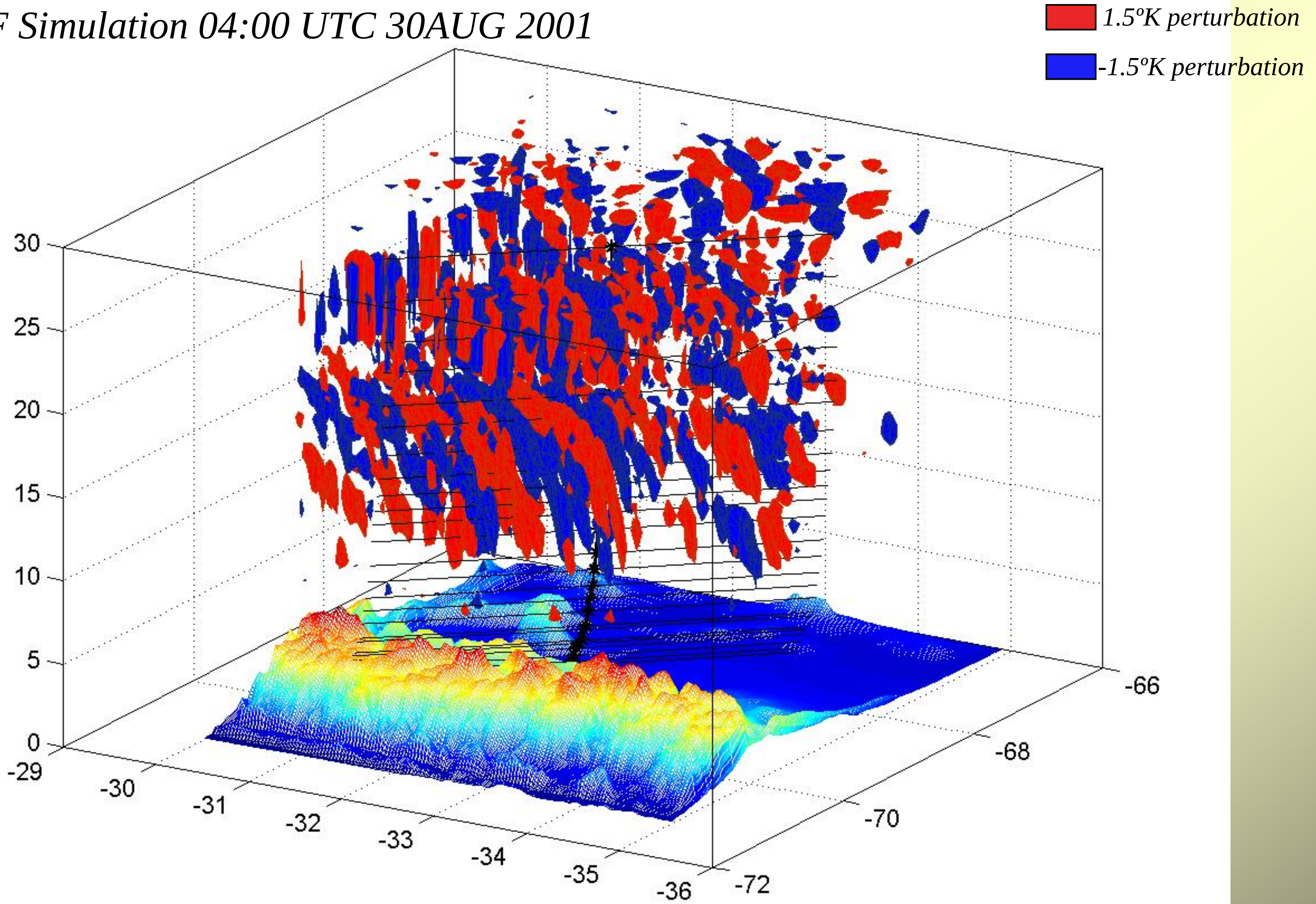

WRF Simulation 04:00 UTC 30AUG 2001

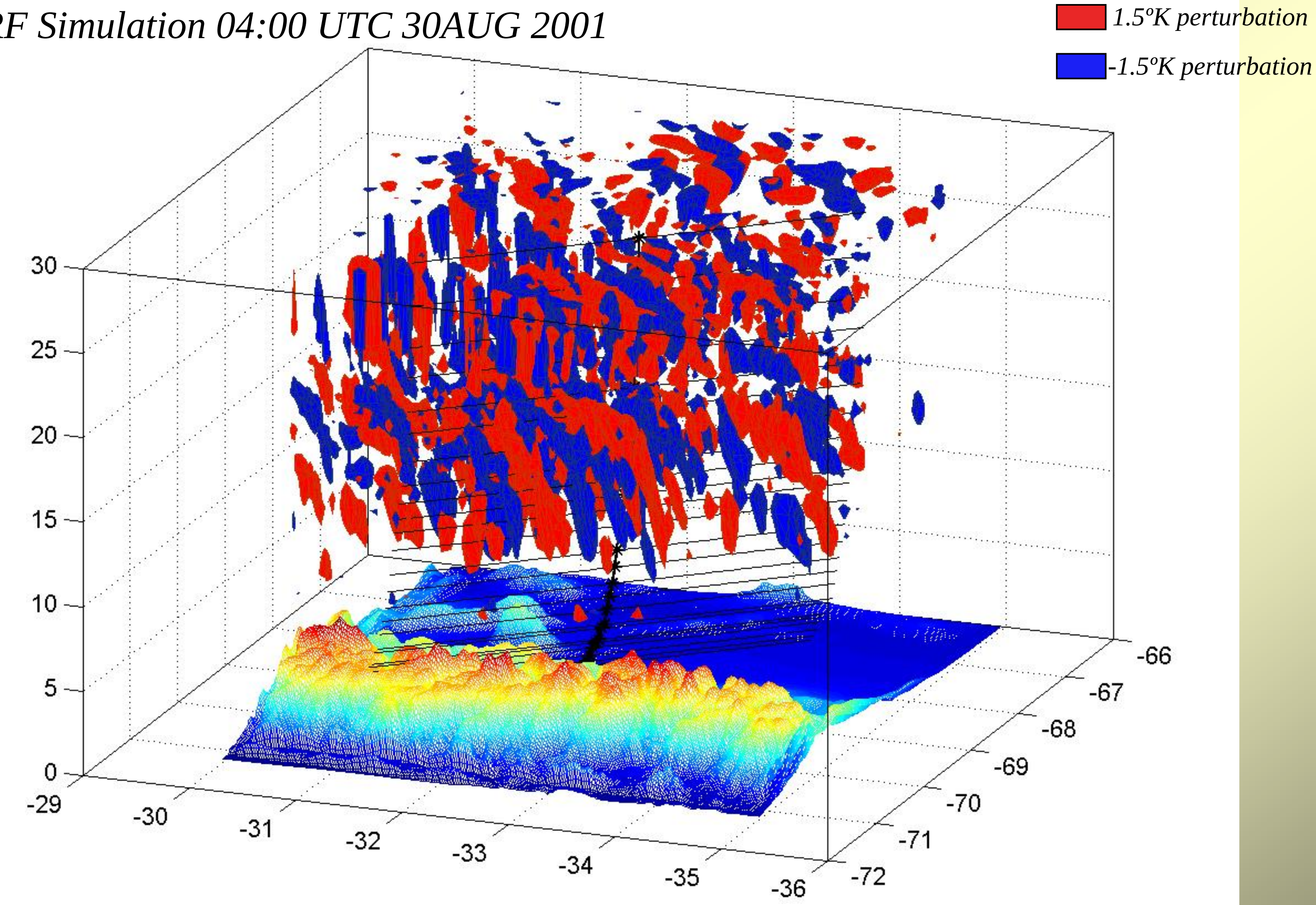

WRF Simulation 04:00 UTC 30AUG 2001

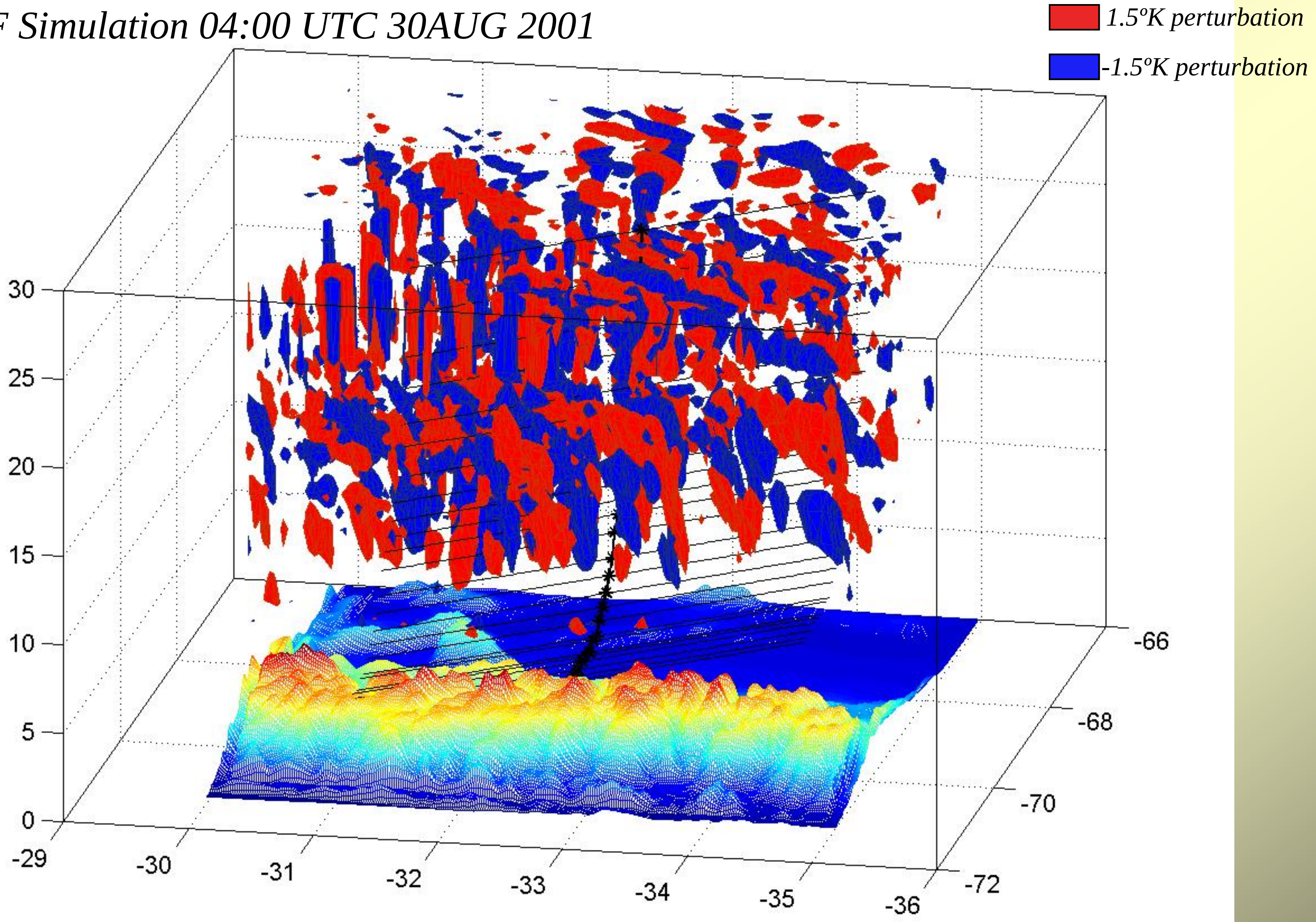

WRF Simulation 04:00 UTC 30AUG 2001

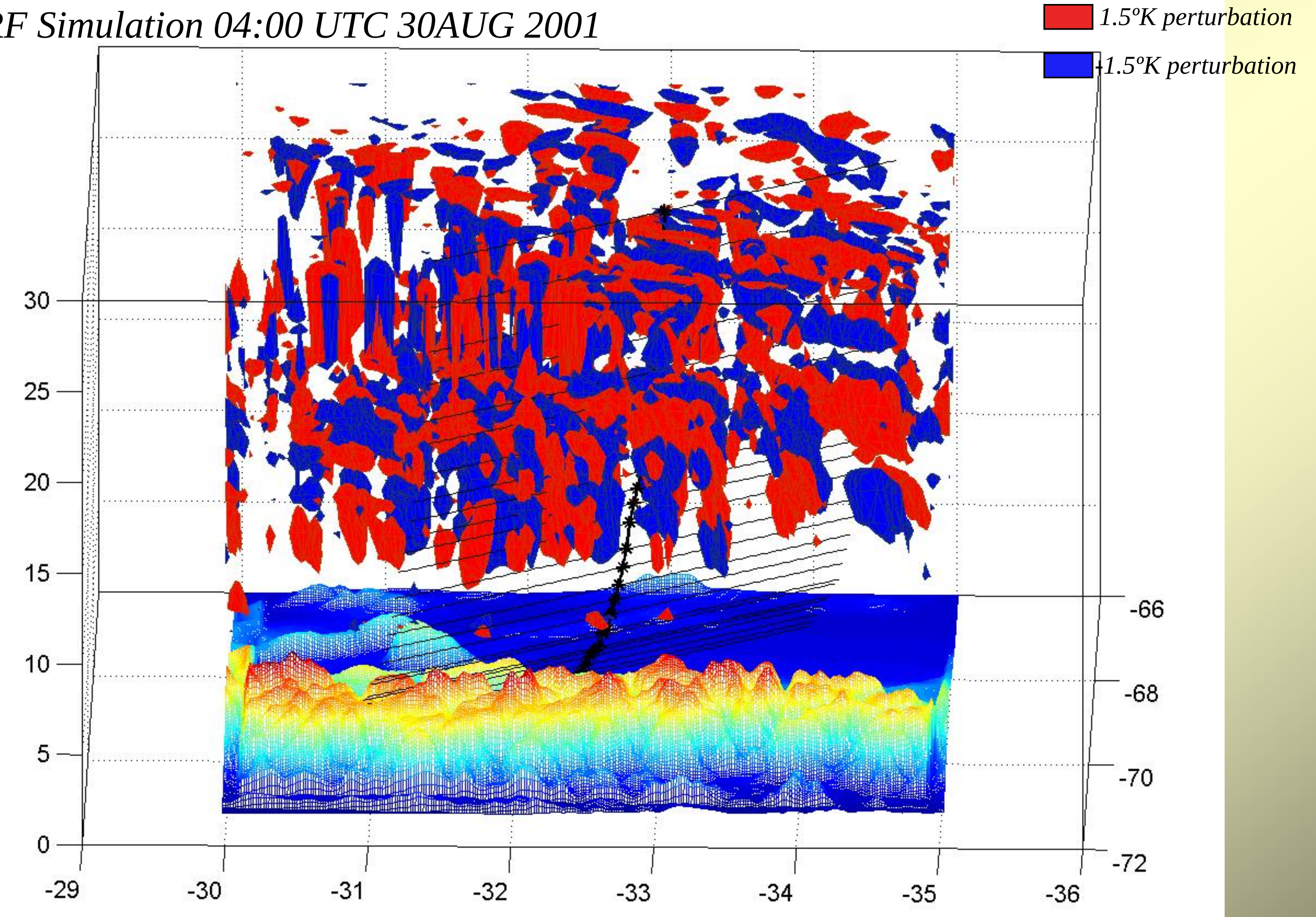

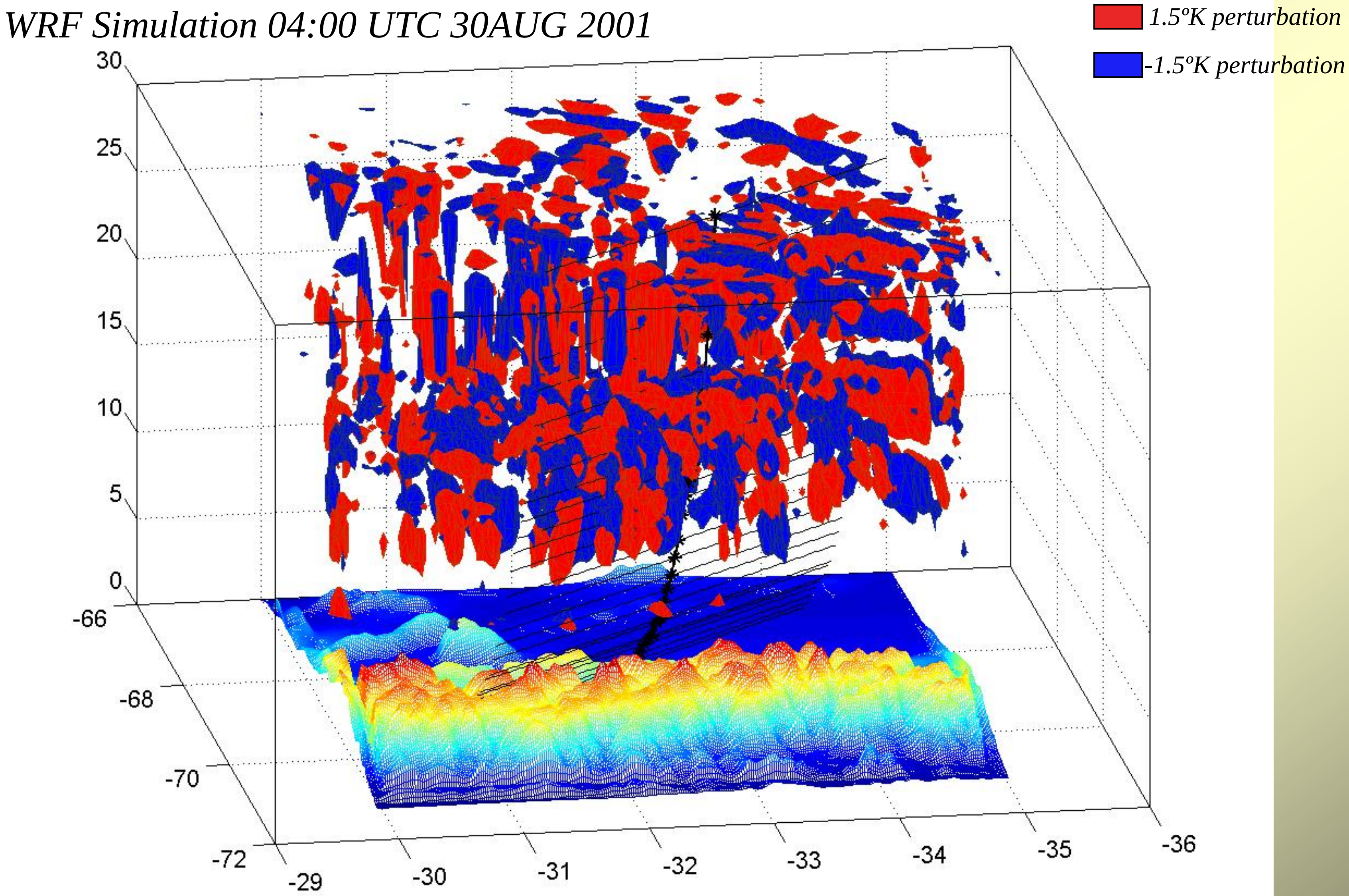

WRF Simulation 04:00 UTC 30AUG 2001
1.5ºK perturbation
-1.5ºK perturbation
30
25
20
15
10
5
0
-66
-68
-70
-72
-29
-30
-31
-32
-33
-34
-35
-36

WRF Simulation 04:00 UTC 30AUG 2001

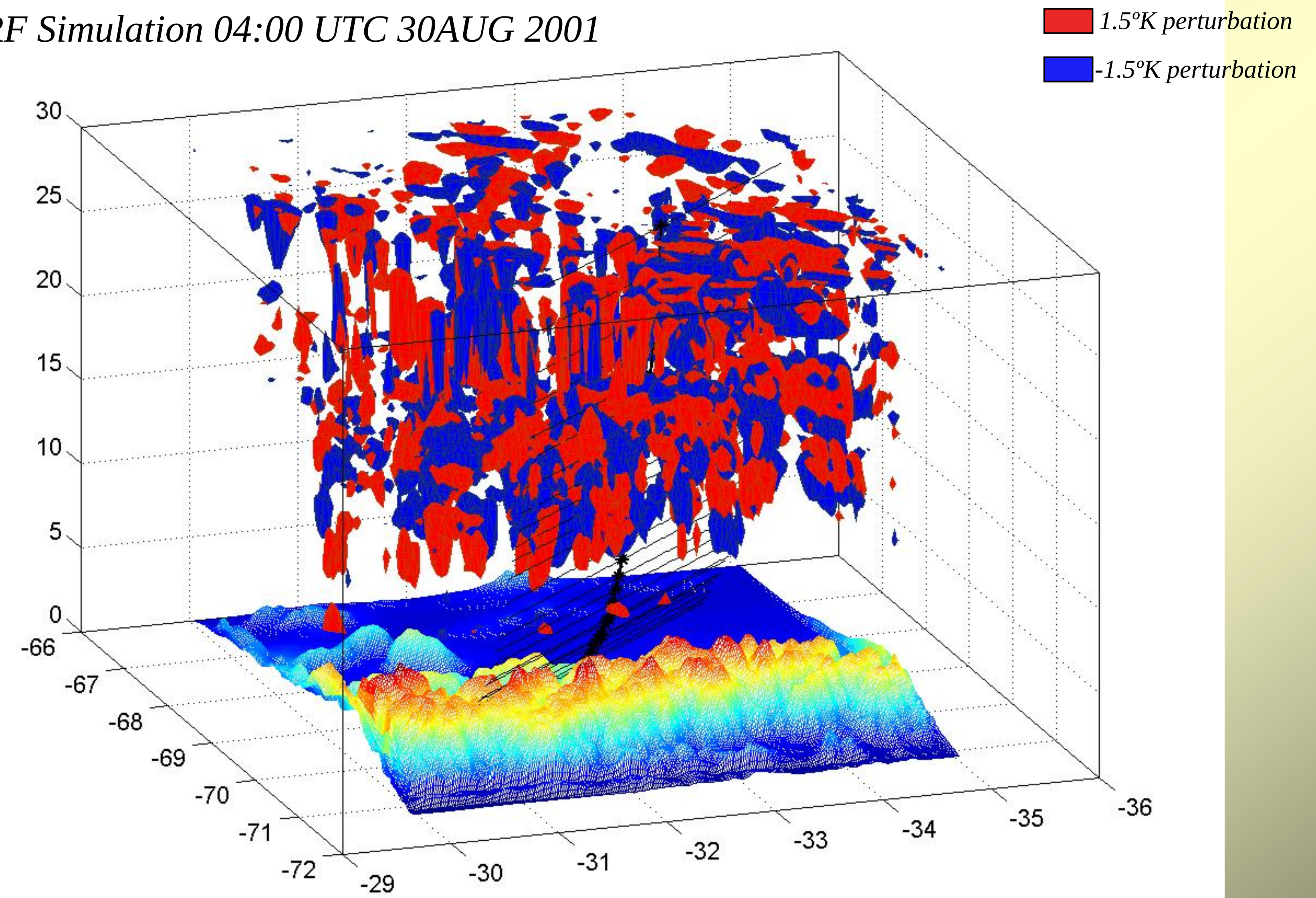

WRF Simulation 04:00 UTC 30AUG 2001

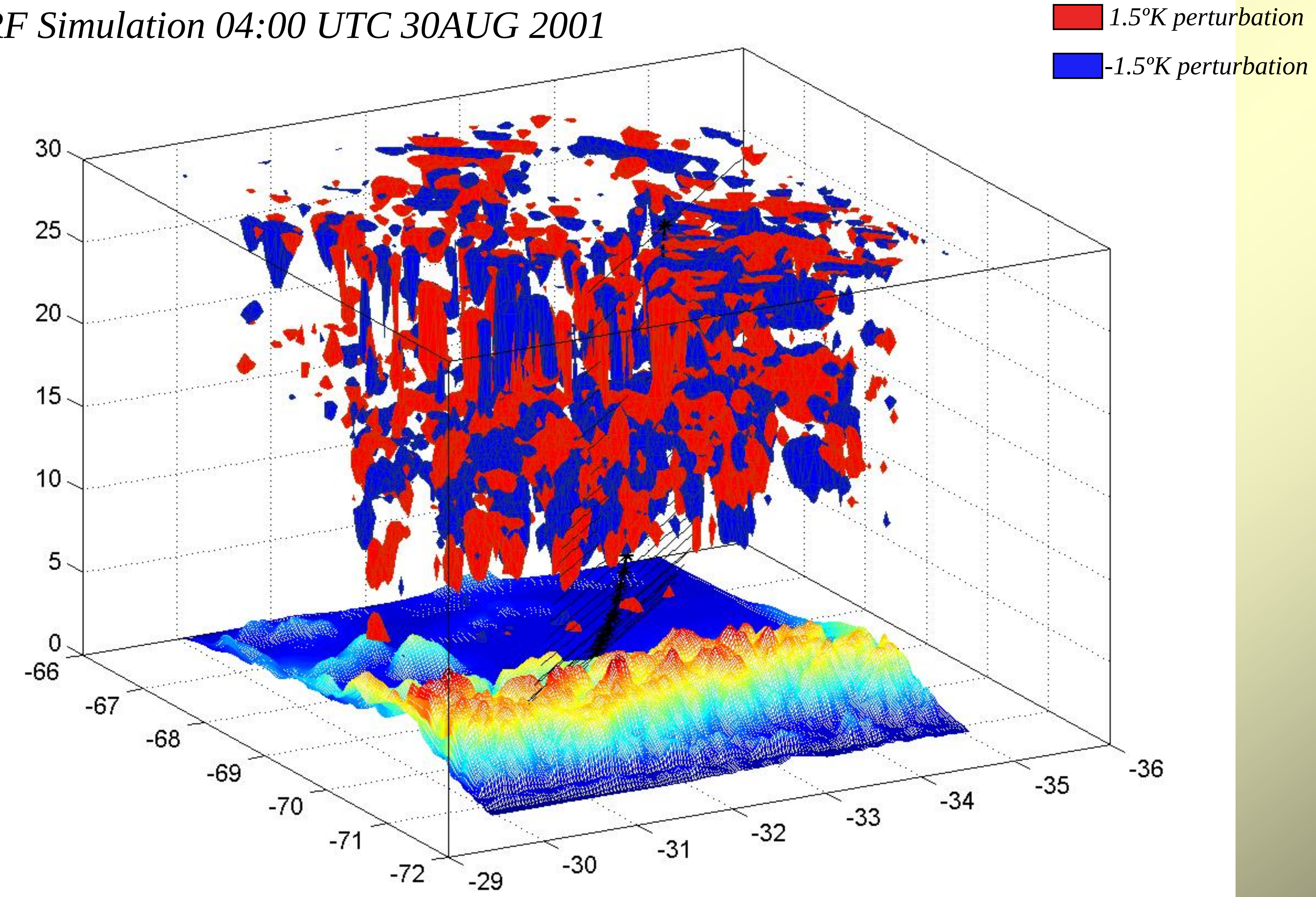

WRF Simulation 04:00 UTC 30AUG 2001

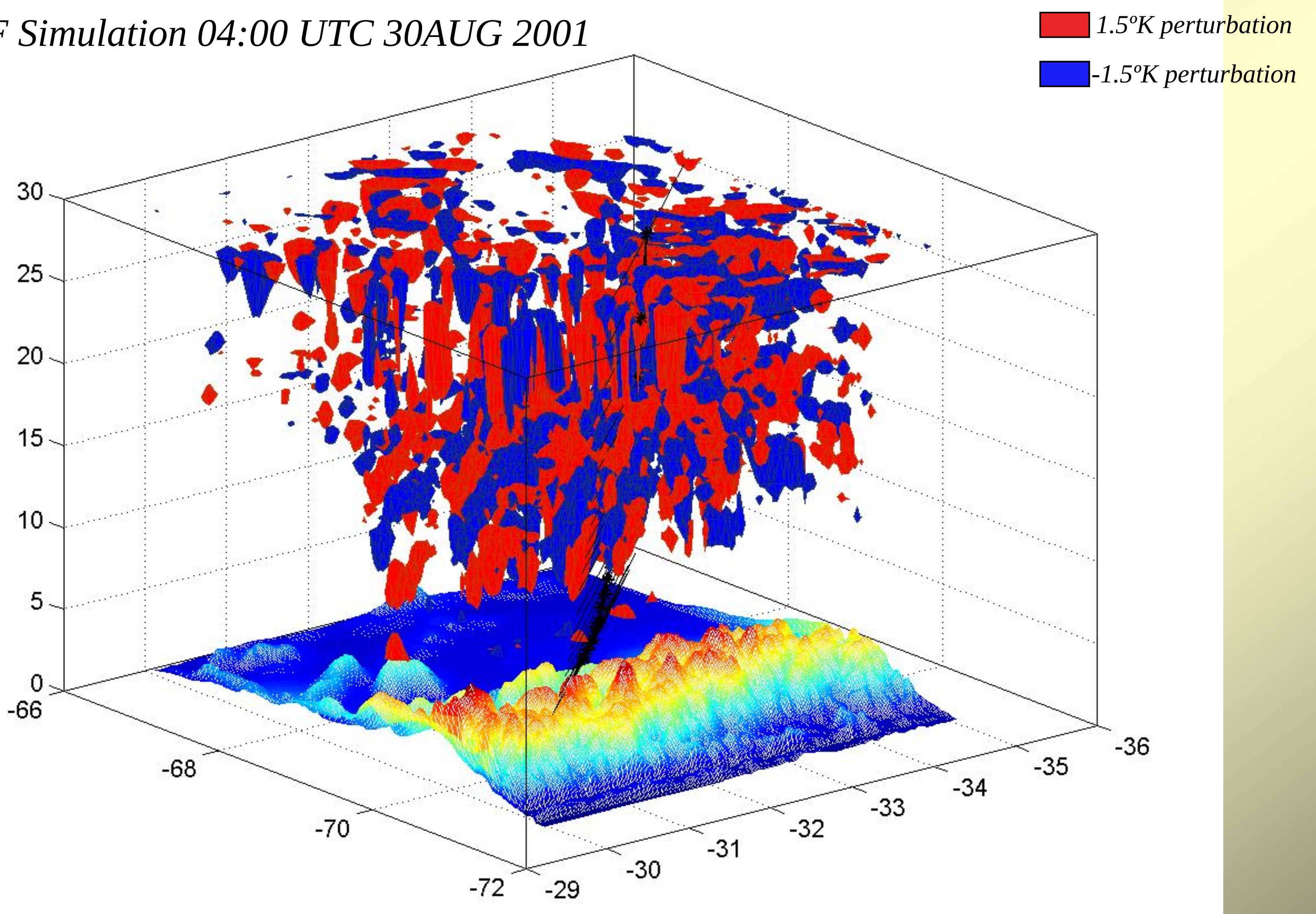

WRF Simulation 04:00 UTC 30AUG 2001

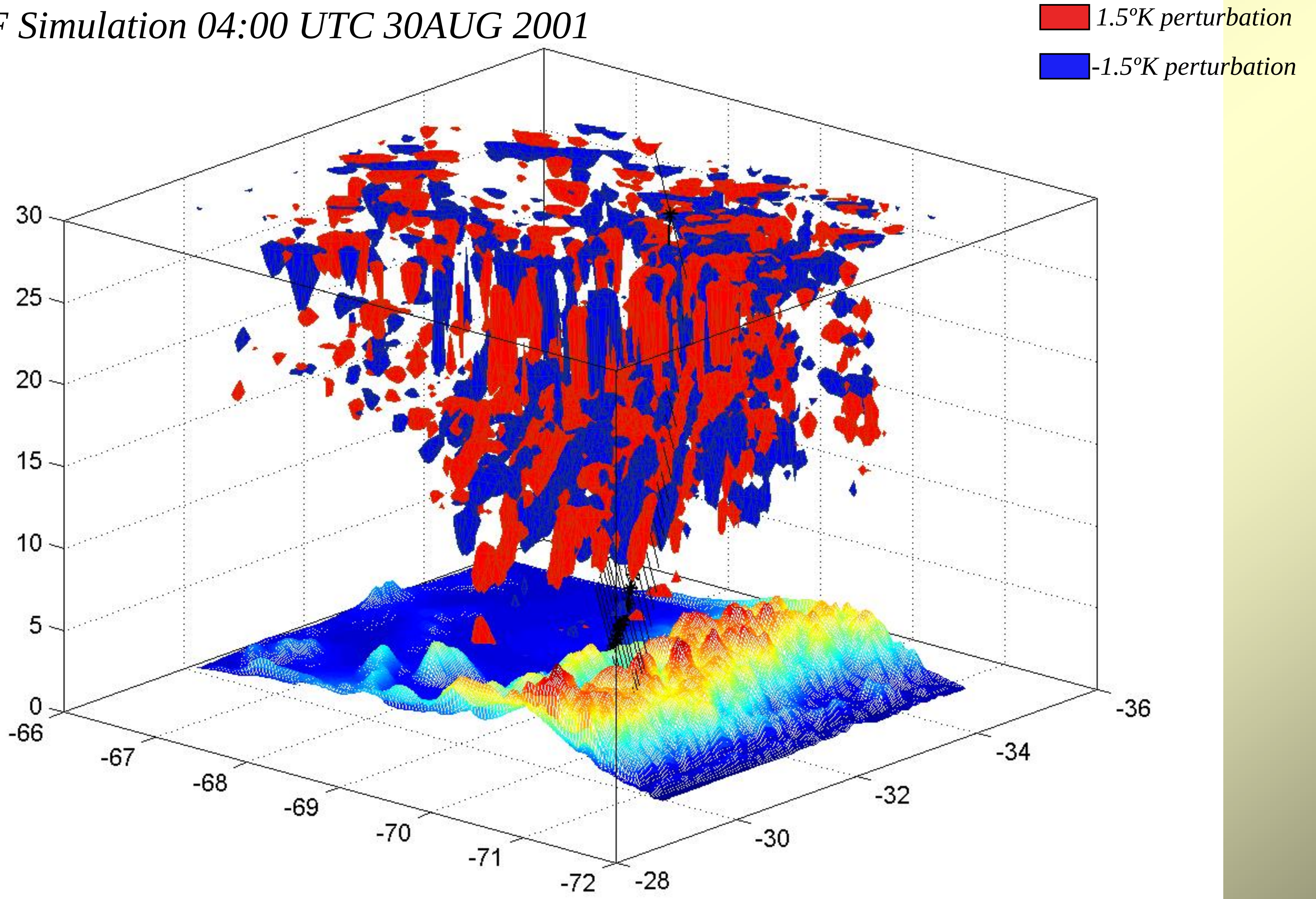

WRF Simulation 04:00 UTC 30AUG 2001

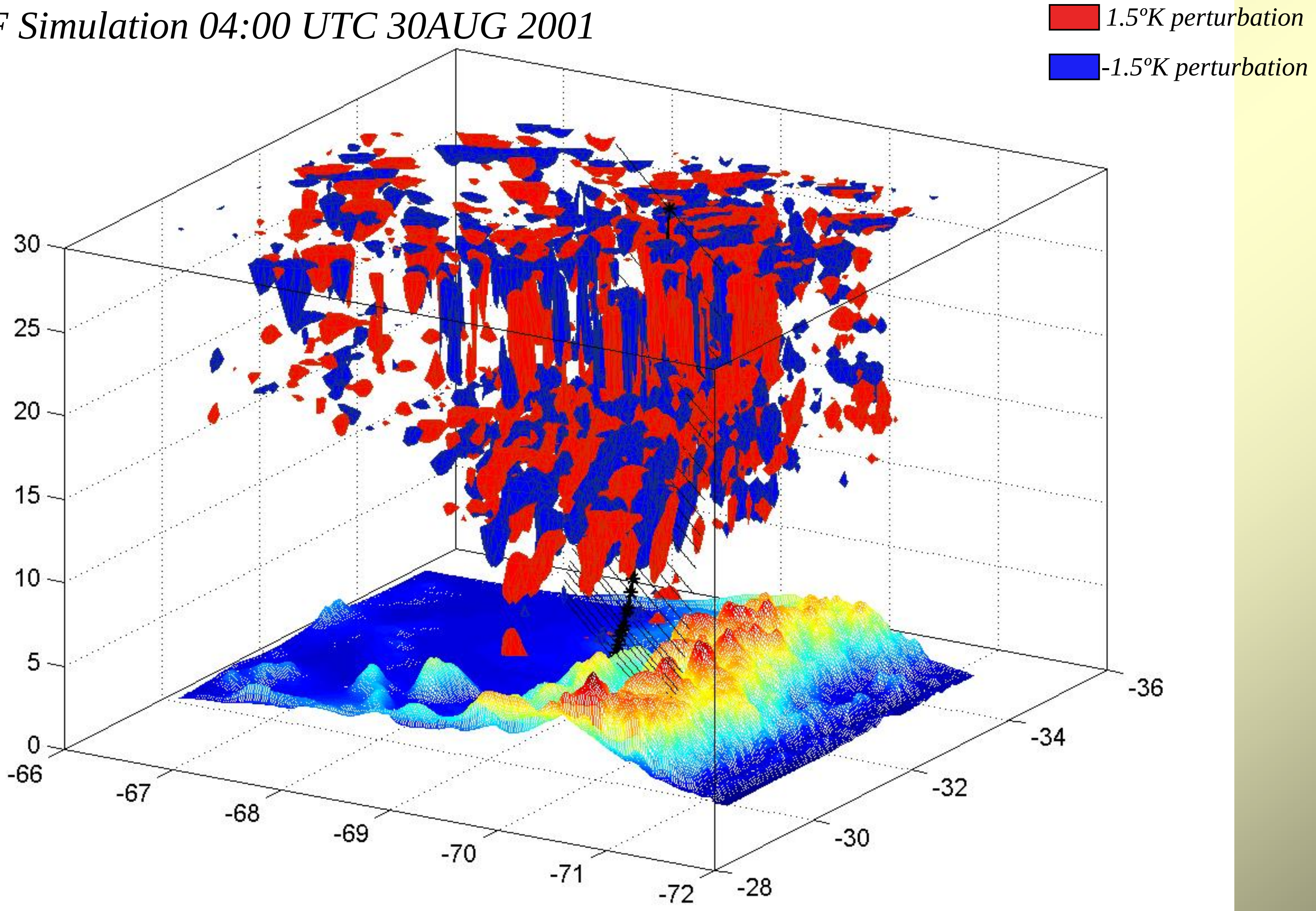

WRF Simulation 04:00 UTC 30AUG 2001

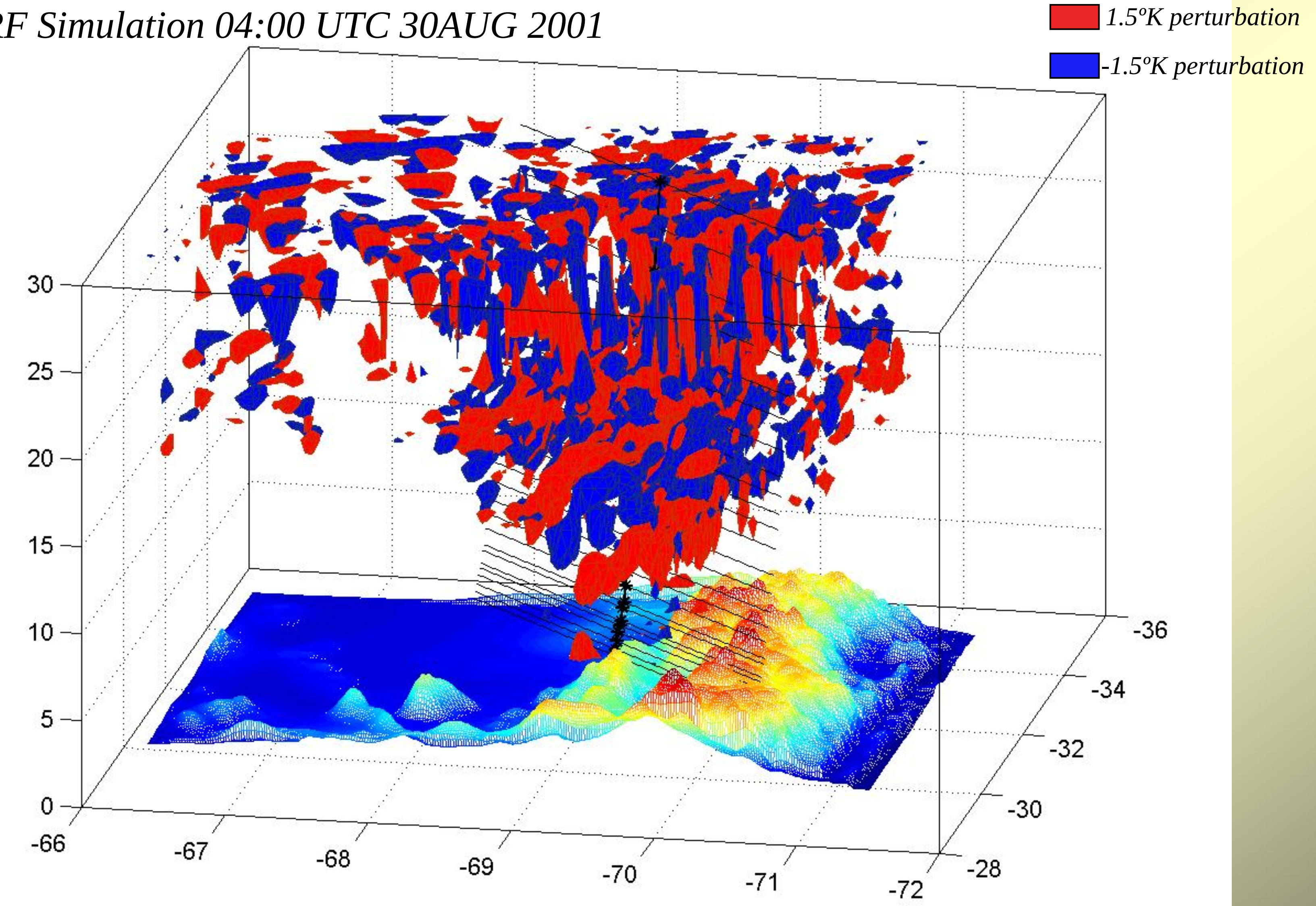

WRF Simulation 04:00 UTC 30AUG 2001

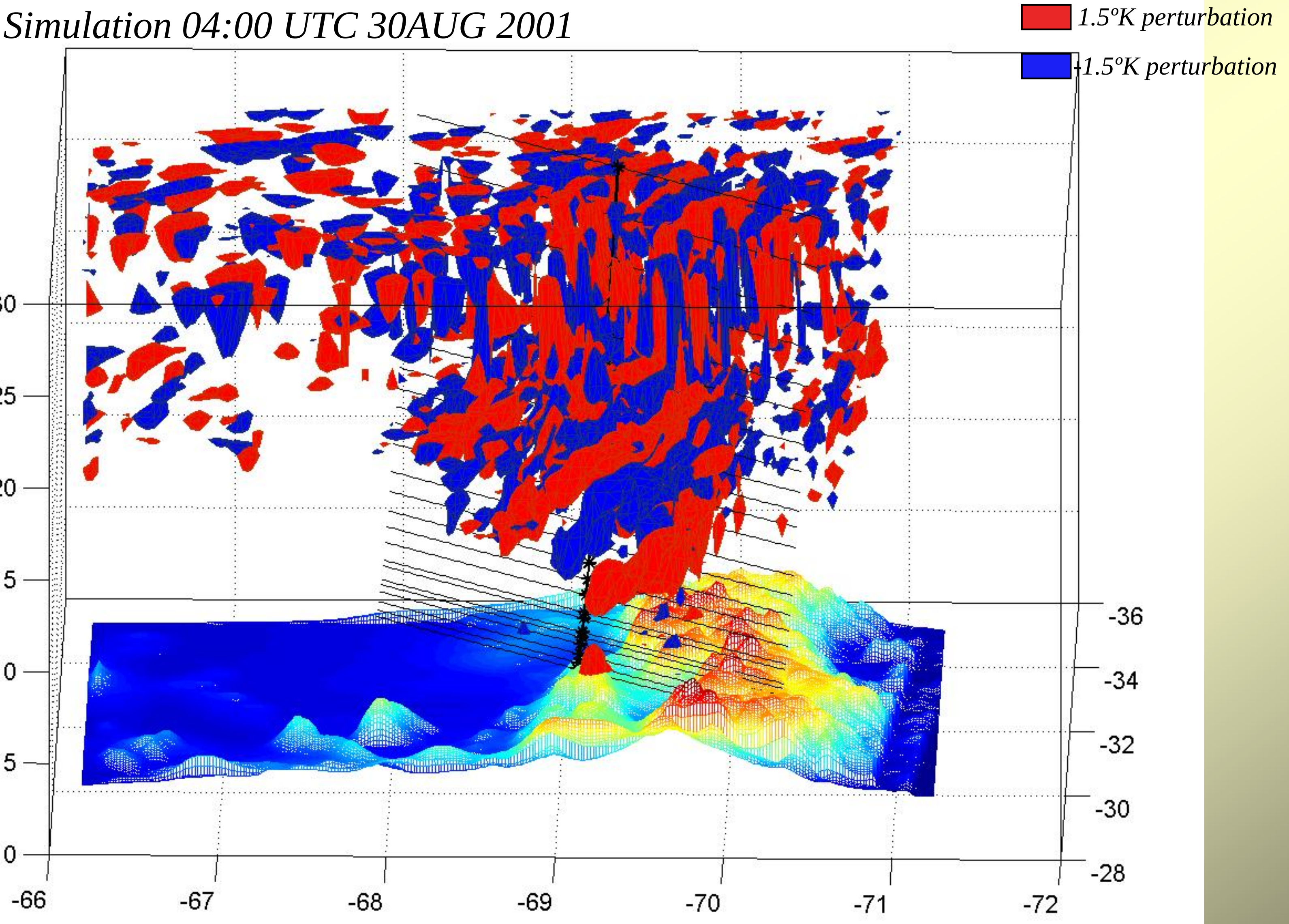

WRF Simulation 04:00 UTC 30AUG 2001

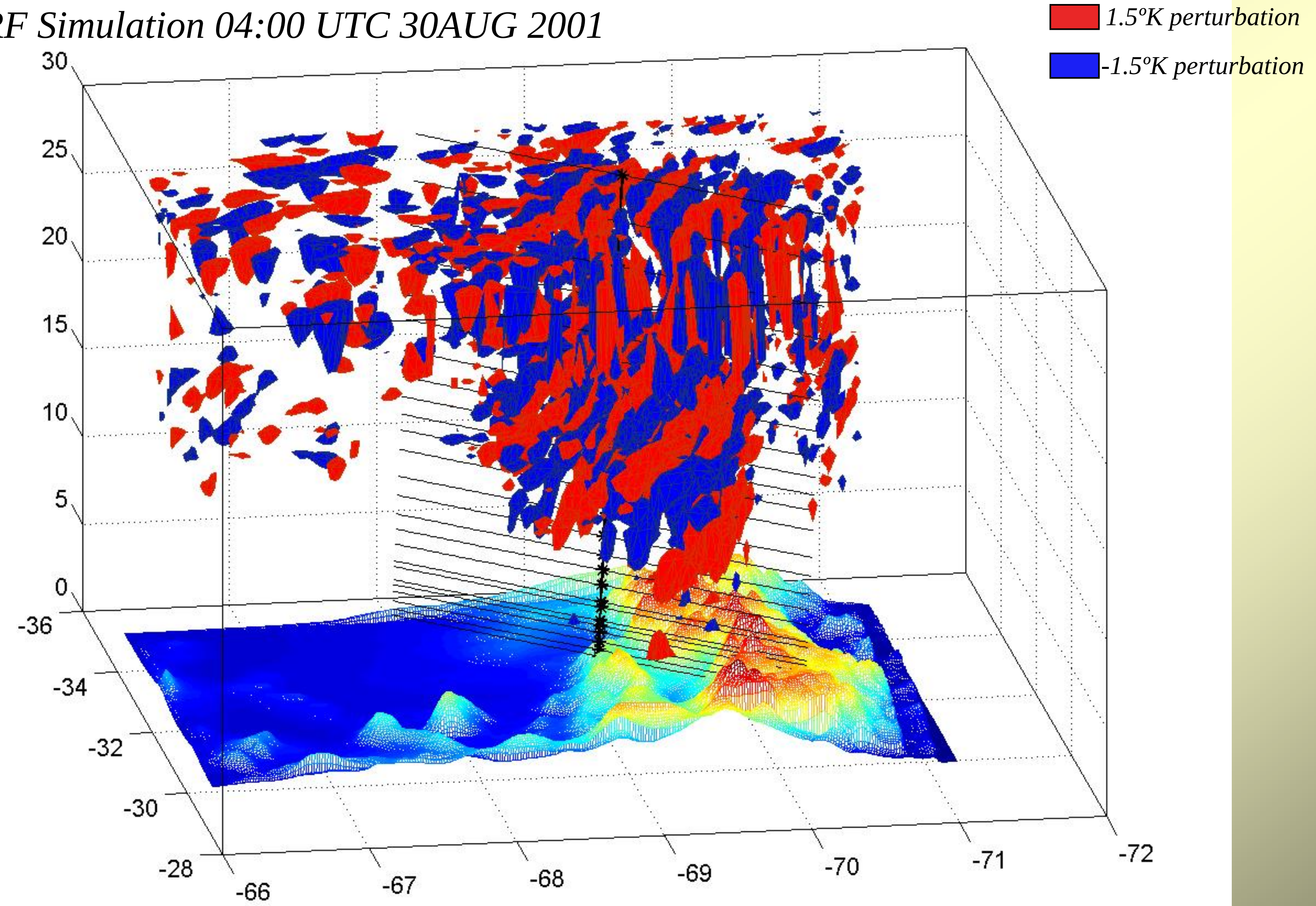

WRF Simulation 04:00 UTC 30AUG 2001

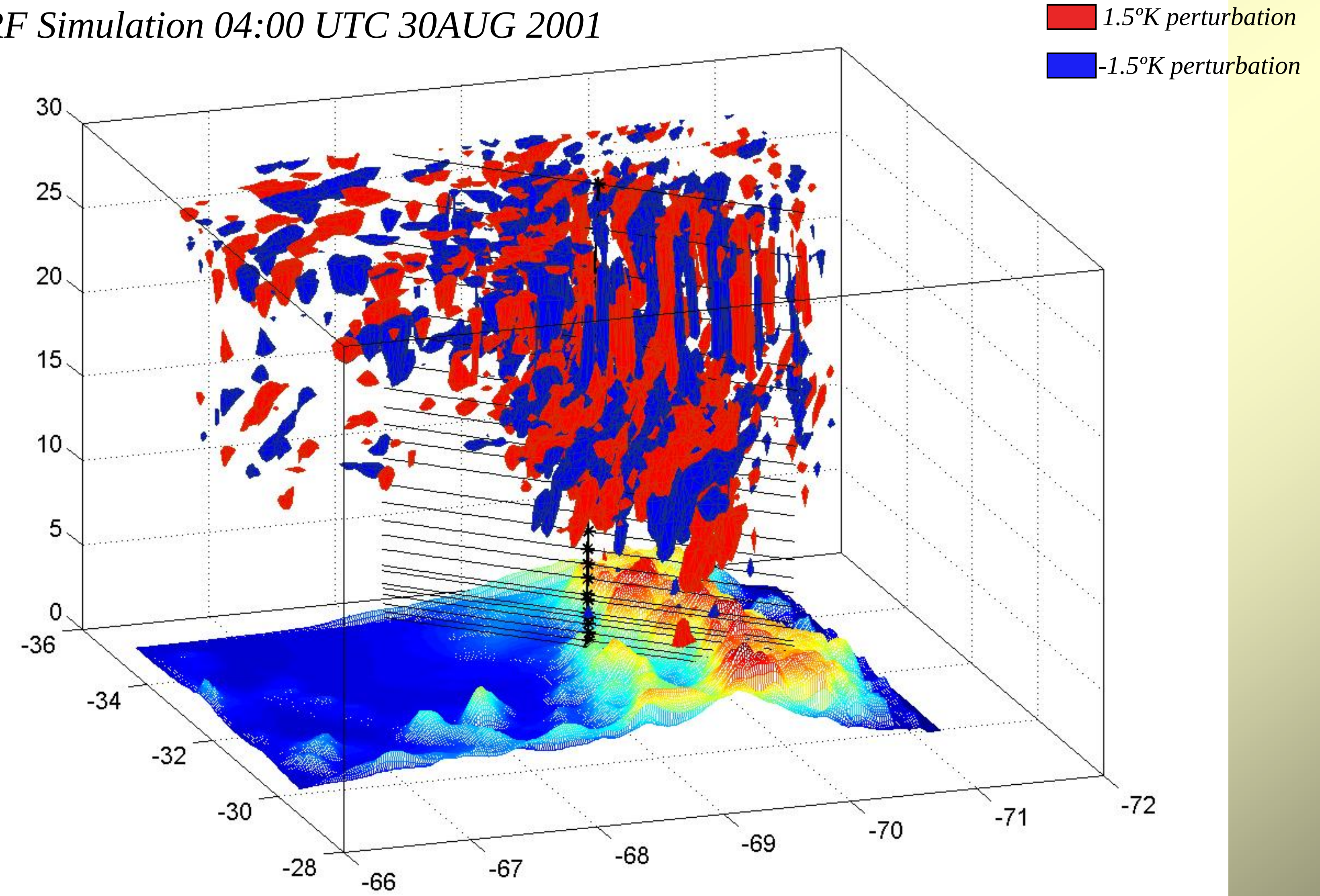

WRF Simulation 04:00 UTC 30AUG 2001

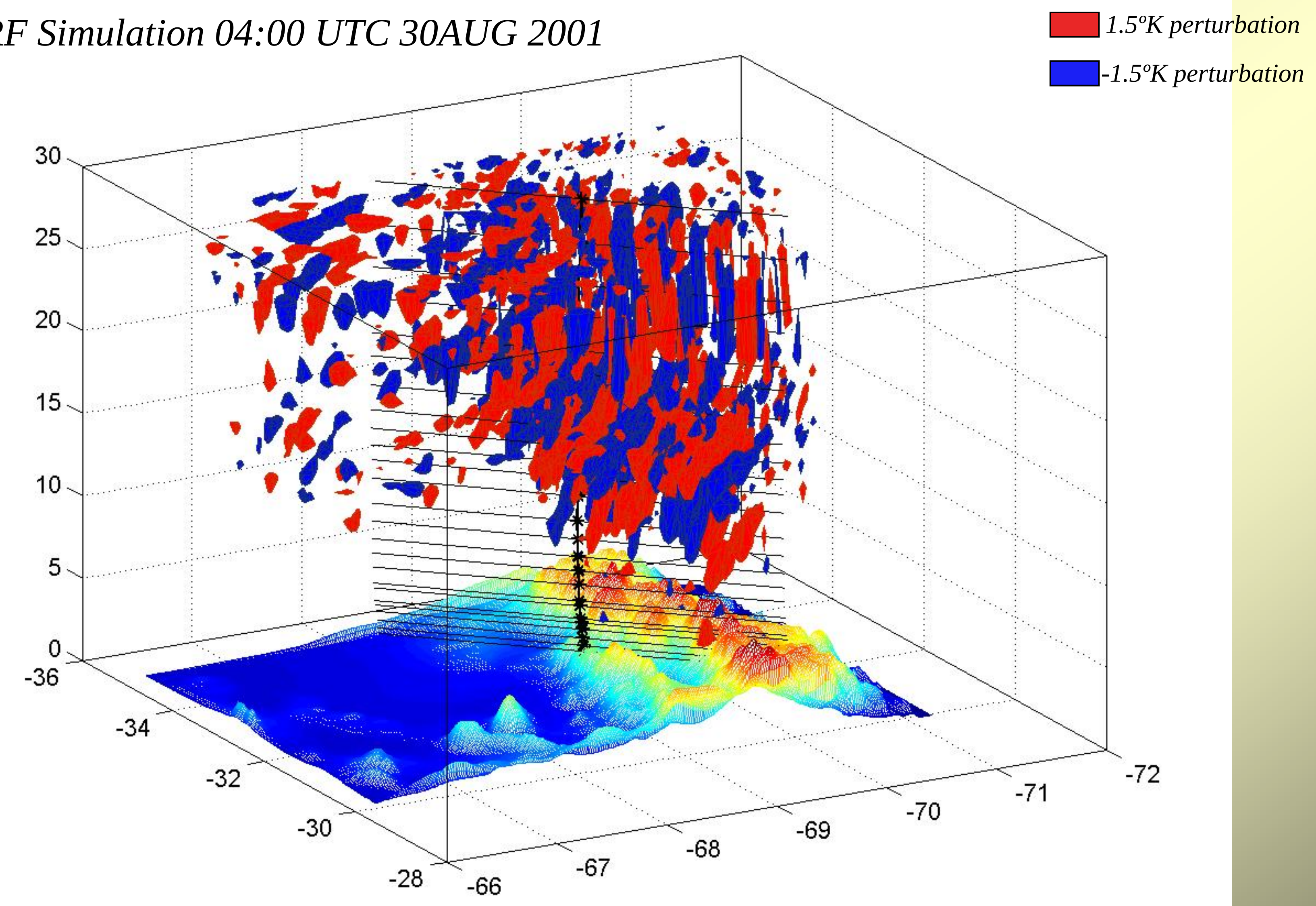

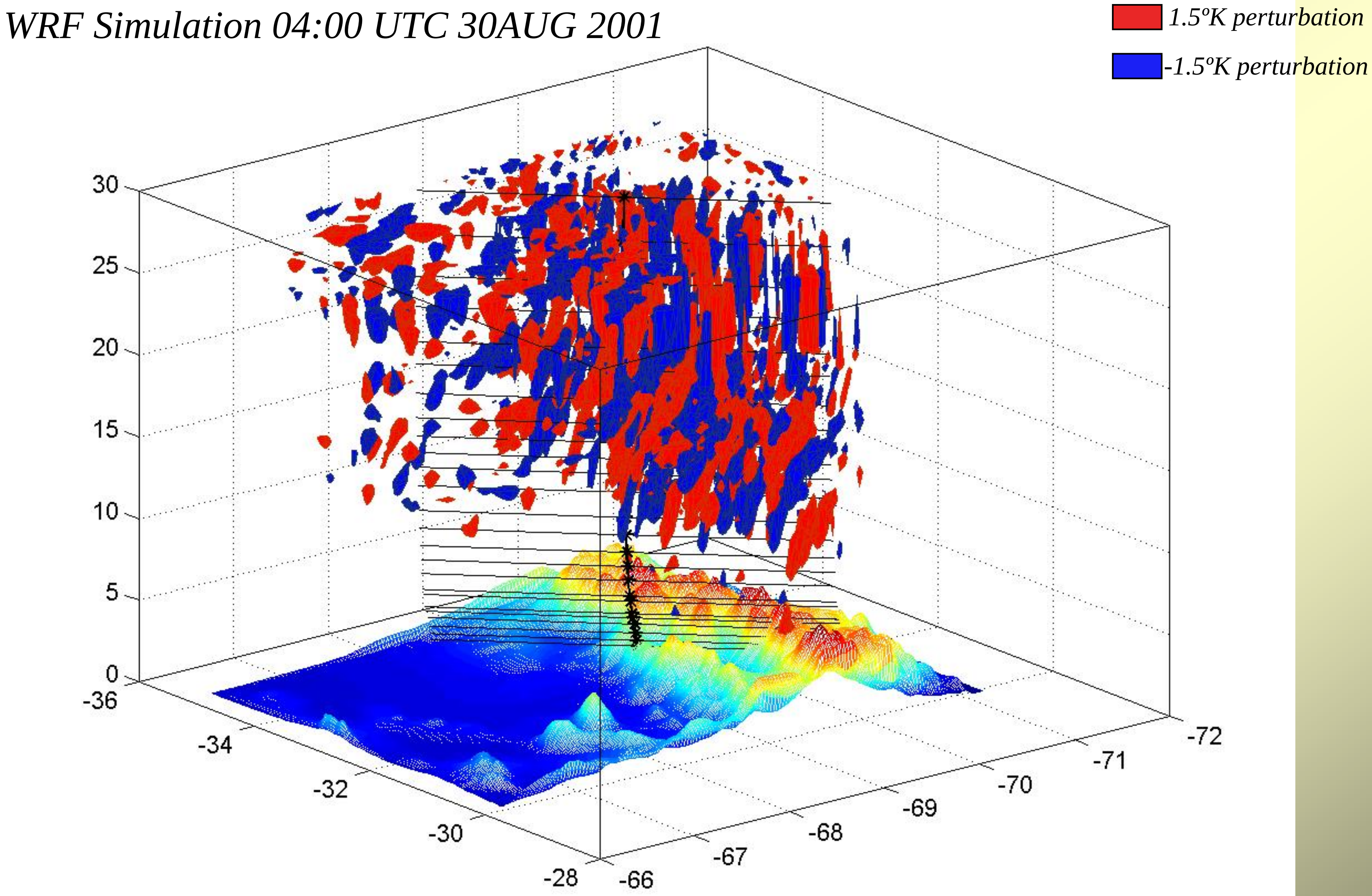
WRF Simulation 04:00 UTC 30AUG 2001
1.5ºK perturbation
-1.5ºK perturbation
30
25
20
15
10
5
0
-36
-34
-32
-30
-28
-66
-67
-68
-69
-70
-71
-72

WRF Simulation 04:00 UTC 30AUG 2001

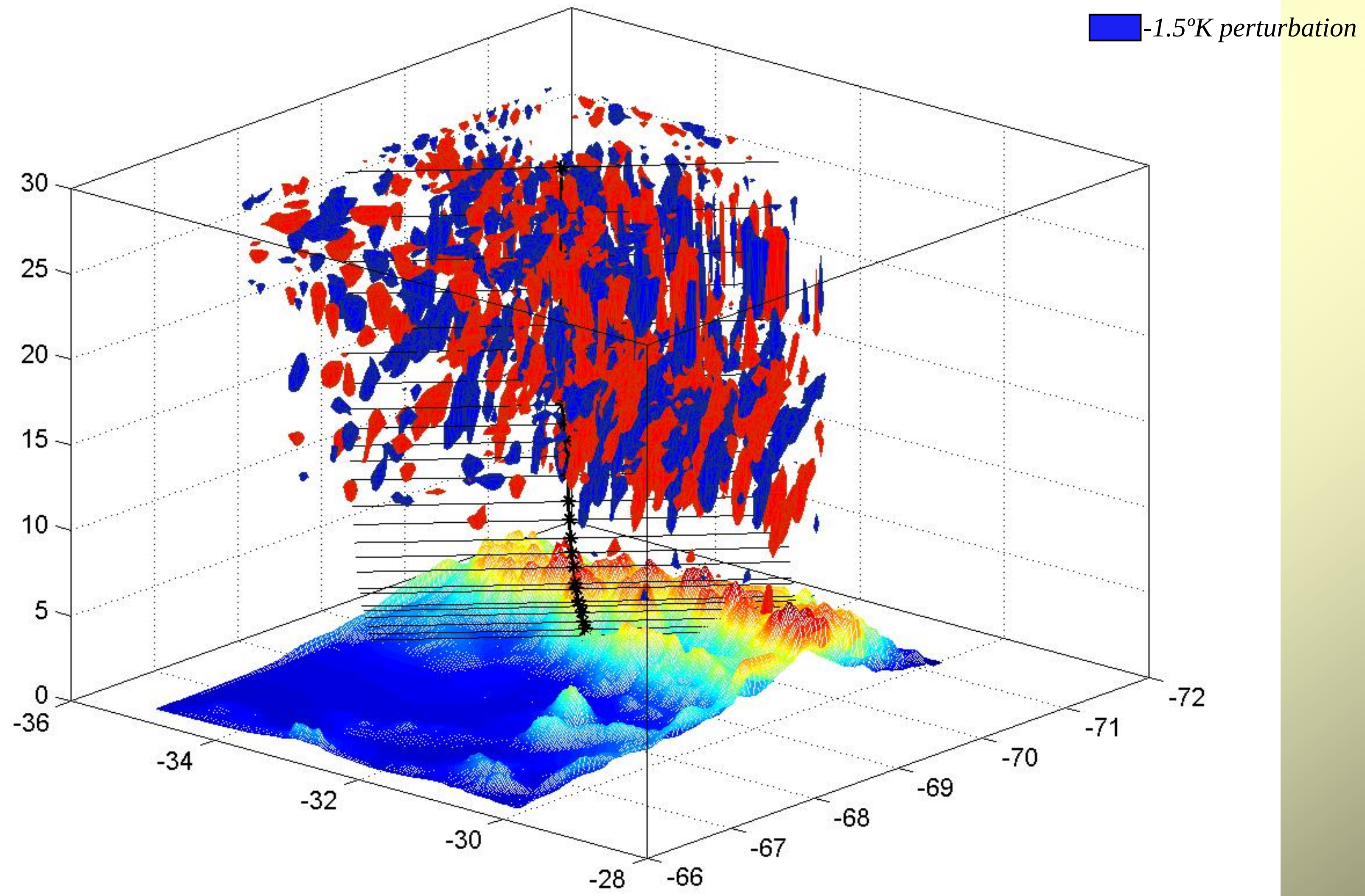

WRF Simulation 04:00 UTC 30AUG 2001

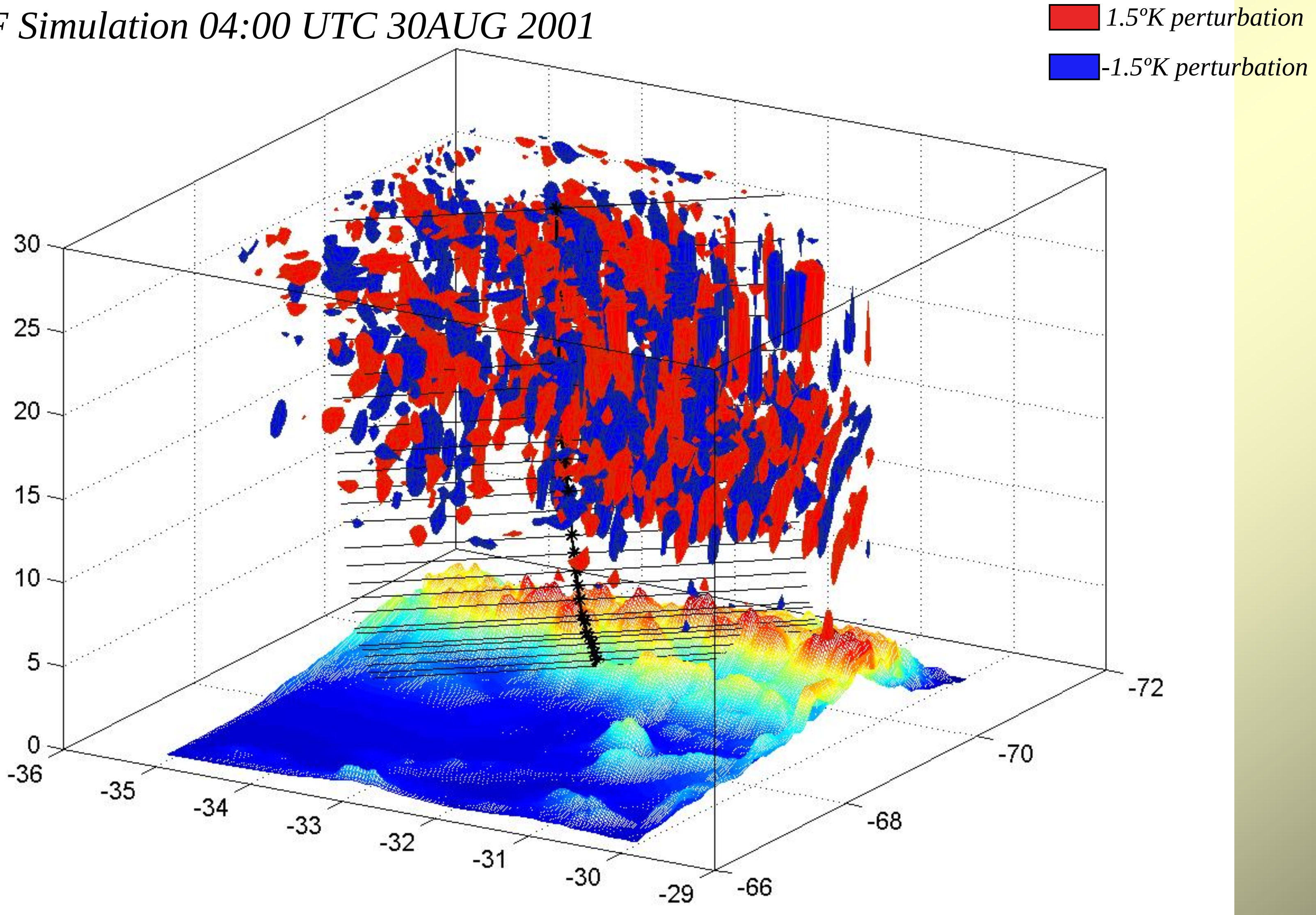

- **In case S2**, the situation is different:

In spite of LTP fell quite far away
from the main WA region,
portions of atmosphere with high WA,
averaged along each LOS,
were partially included:

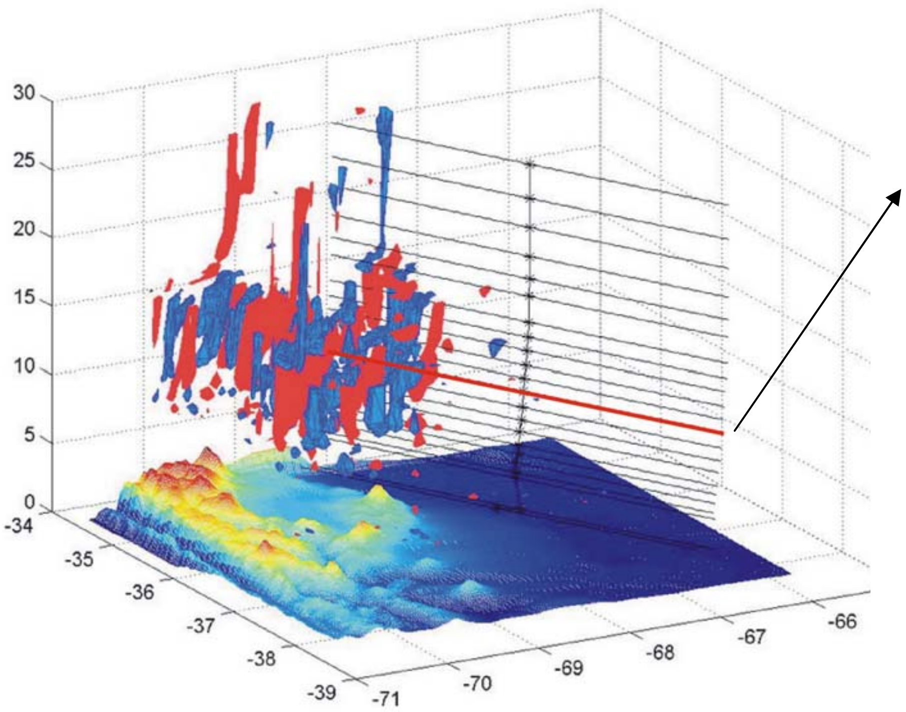

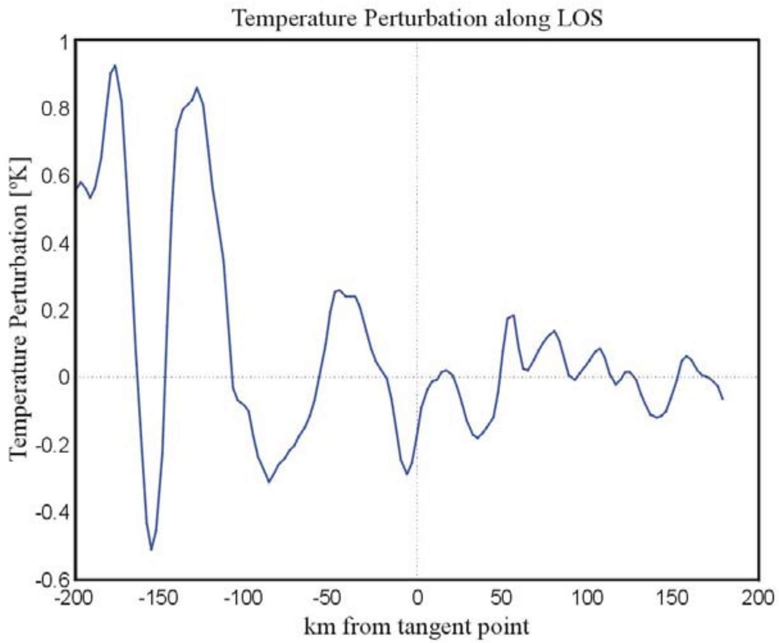

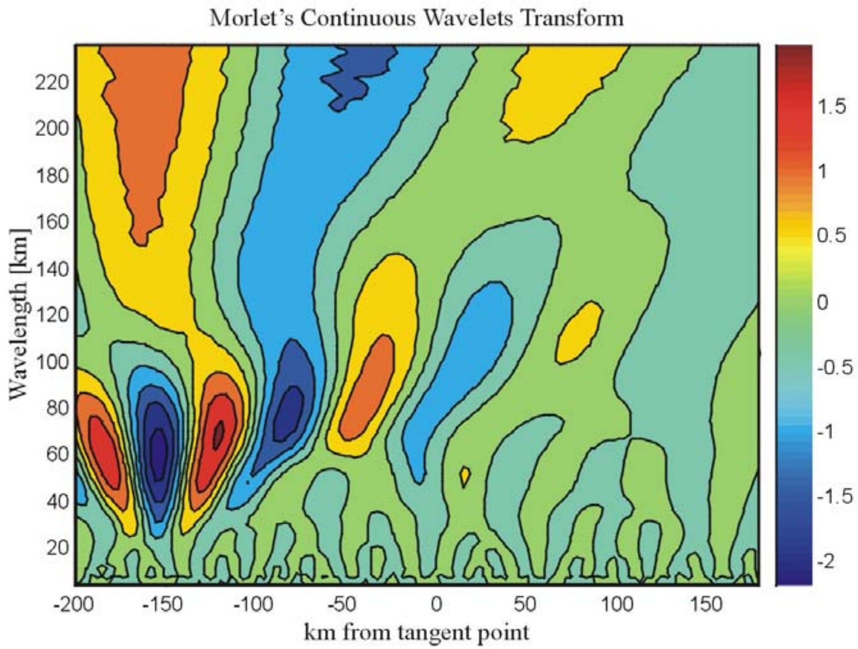

WRF Simulation 04:00 UTC 20NOV 2001

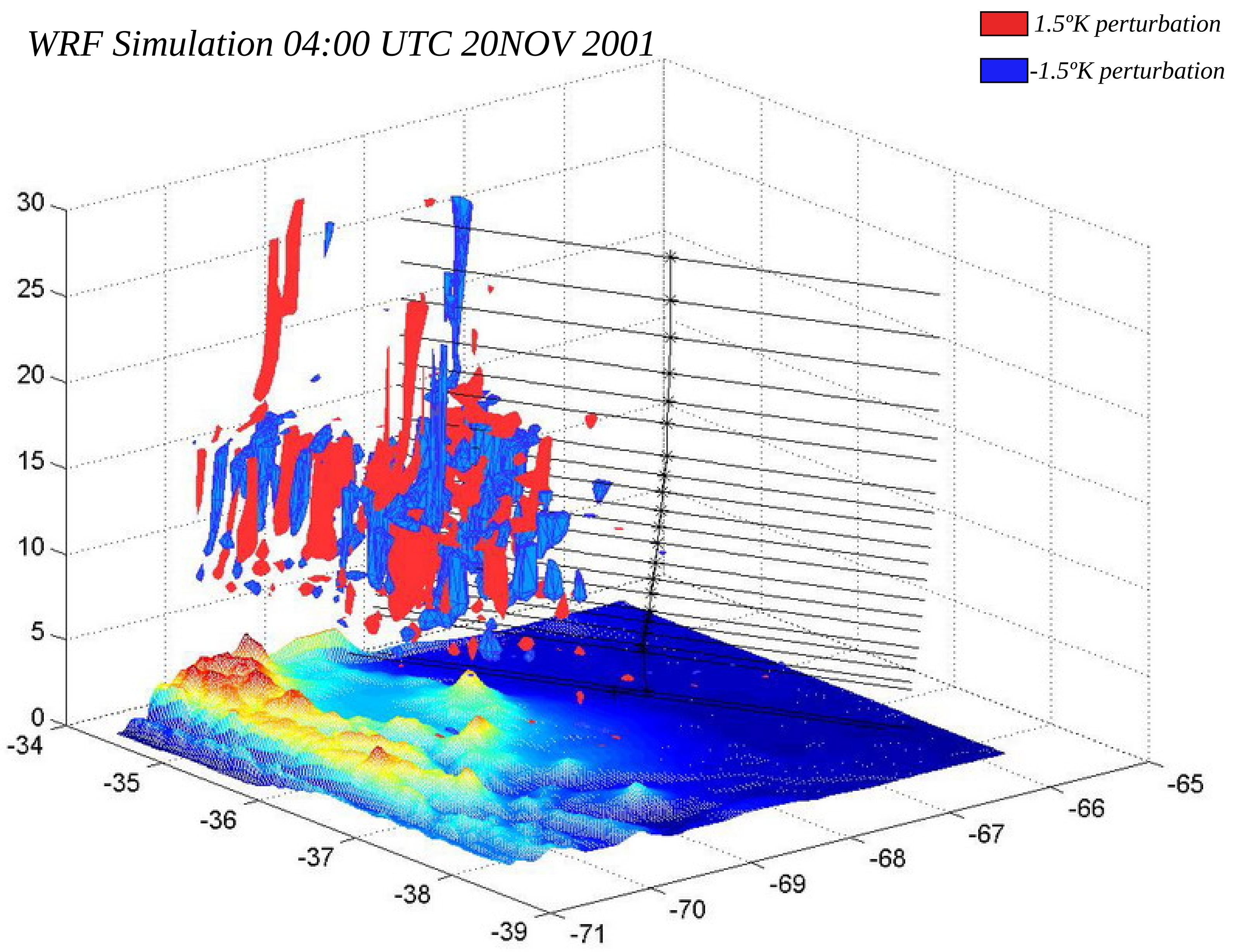

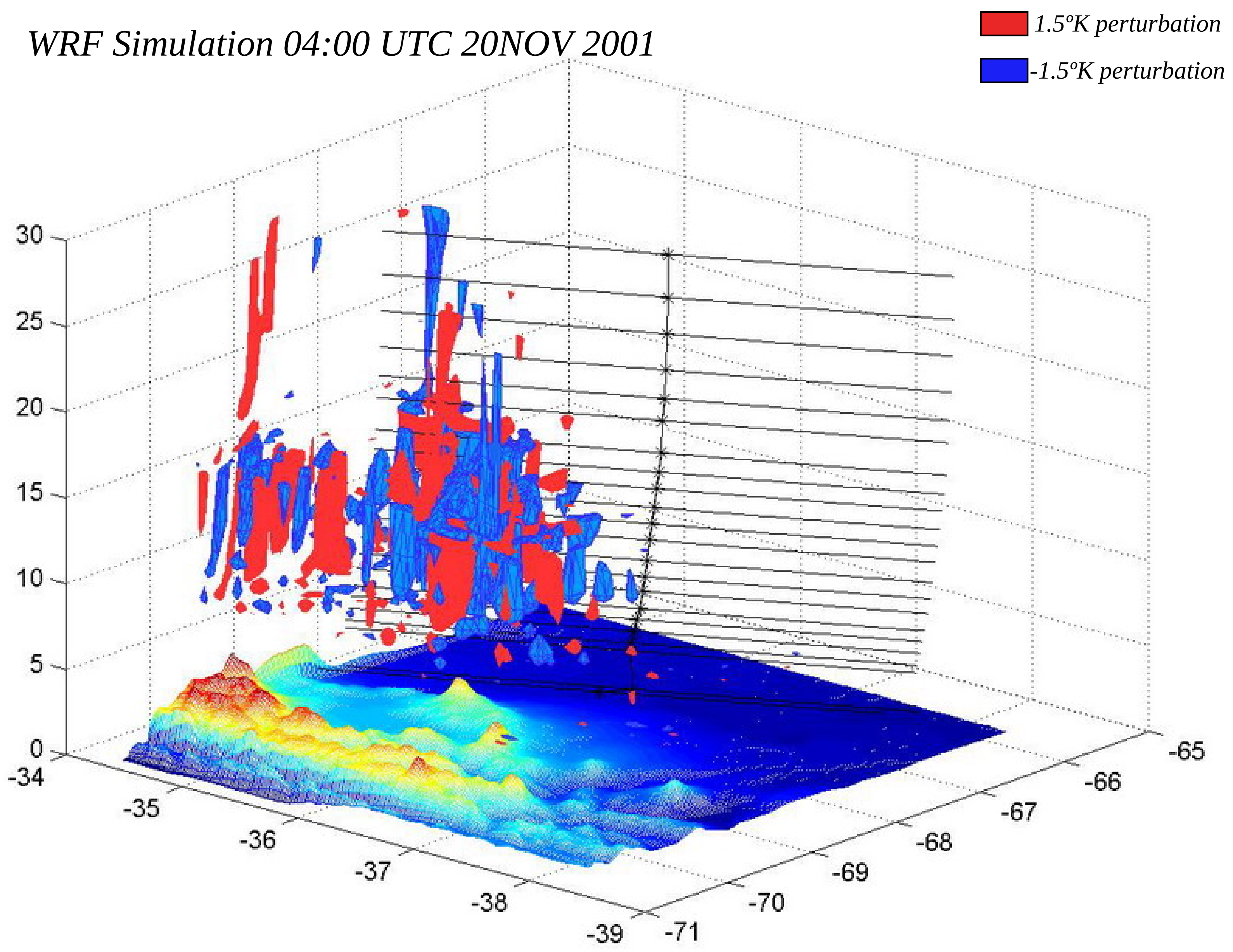
WRF Simulation 04:00 UTC 20NOV 2001
1.5ºK perturbation
-1.5ºK perturbation
30
25
20
15
10
5
0
-34
-35
-36
-37
-38
-39
-71
-70
-69
-68
-67
-66
-65

WRF Simulation 04:00 UTC 20NOV 2001

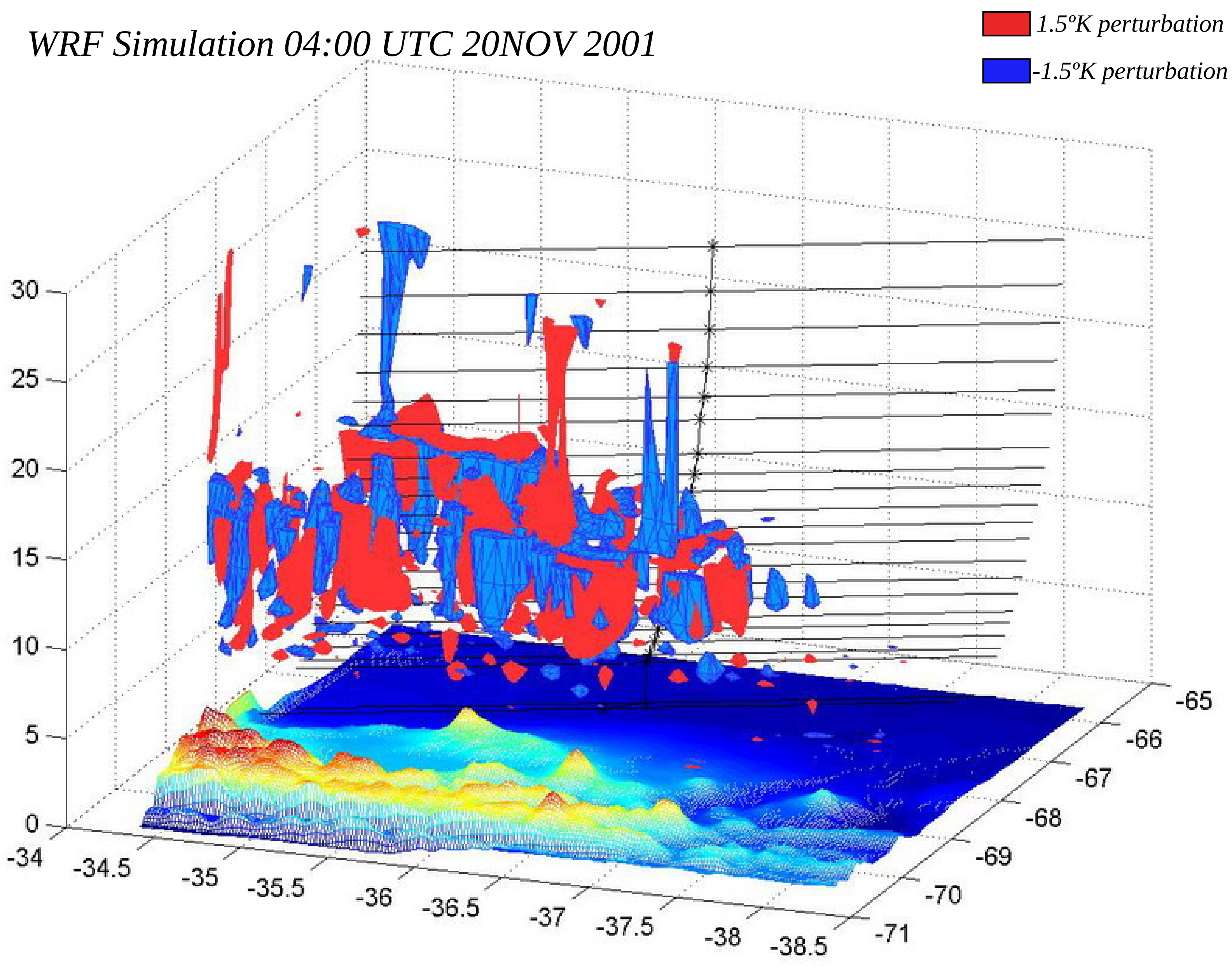

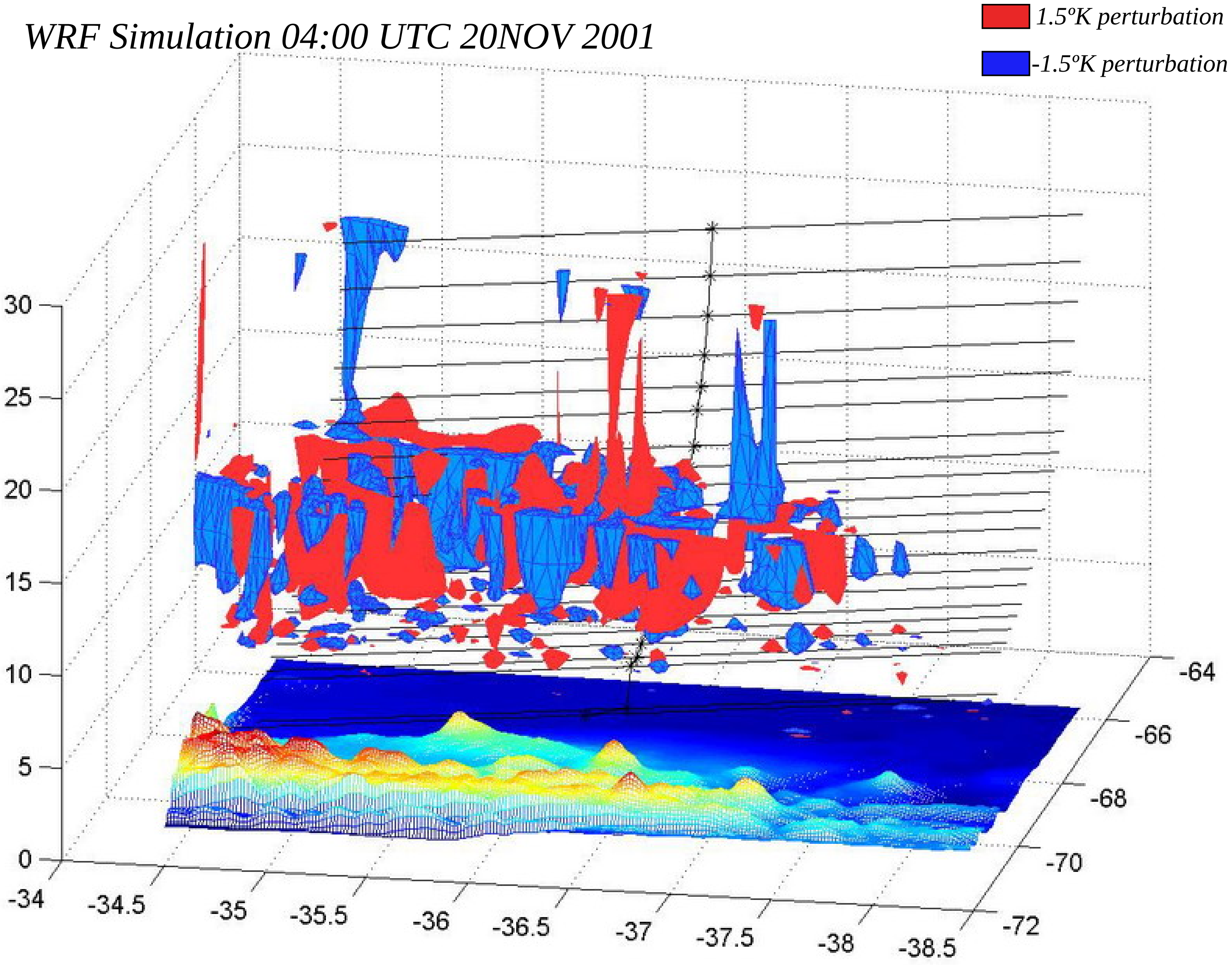

WRF Simulation 04:00 UTC 20NOV 2001
1.5ºK perturbation
-1.5ºK perturbation
30
25
20
15
10
5
0
-34
-34.5
-35
-35.5
-36
-36.5
-37
-37.5
-38
-38.5
-64
-66
-68
-70
-72

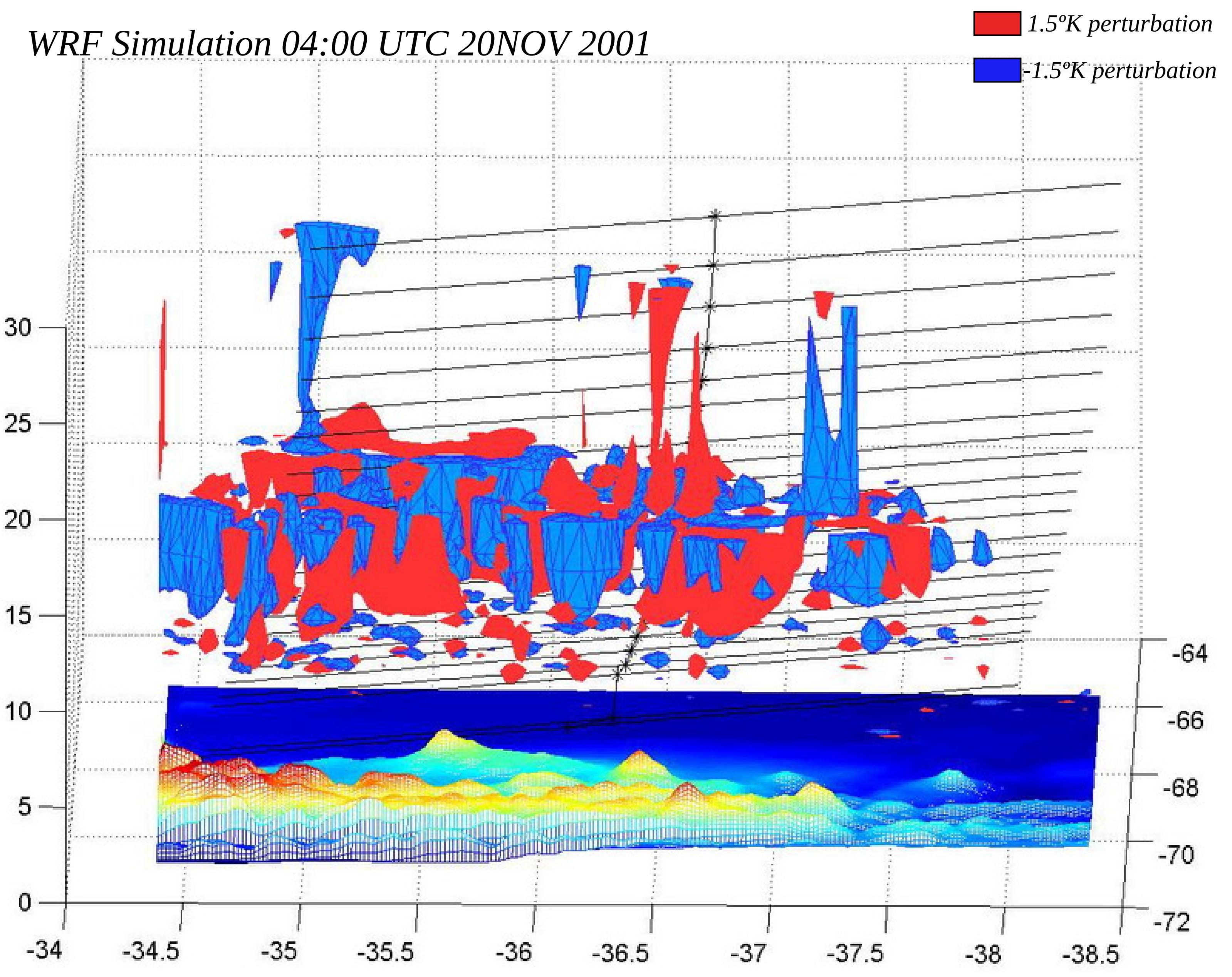
WRF Simulation 04:00 UTC 20NOV 2001
1.5ºK perturbation
-1.5ºK perturbation
30
25
20
15
10
5
0
-34
-34.5
-35
-35.5
-36
-36.5
-37
-37.5
-38
-38.5
-64
-66
-68
-70
-72

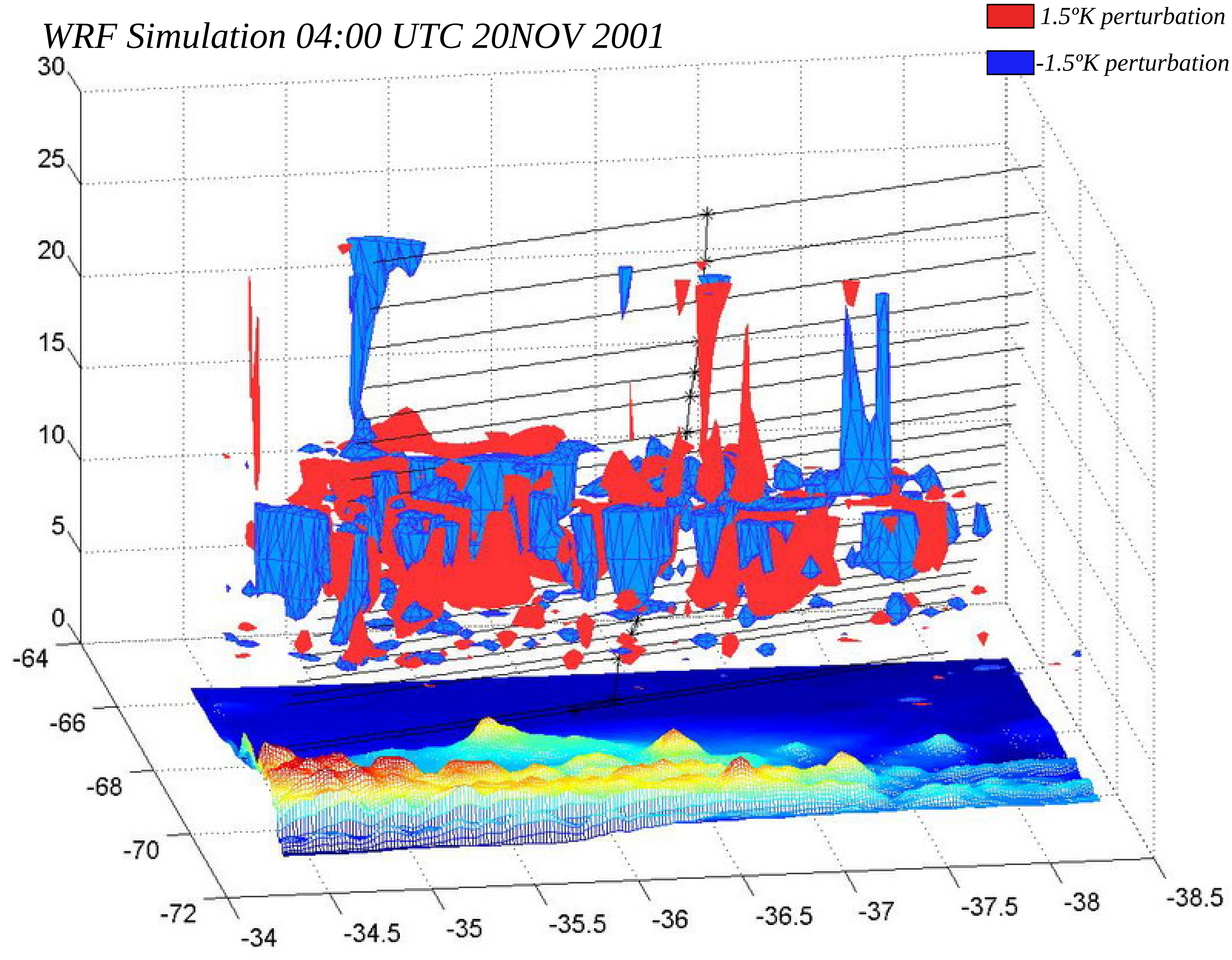
WRF Simulation 04:00 UTC 20NOV 2001
1.5ºK perturbation
-1.5ºK perturbation
30
25
20
15
10
5
0
-64
-66
-68
-70
-72
-34
-34.5
-35
-35.5
-36
-36.5
-37
-37.5
-38
-38.5

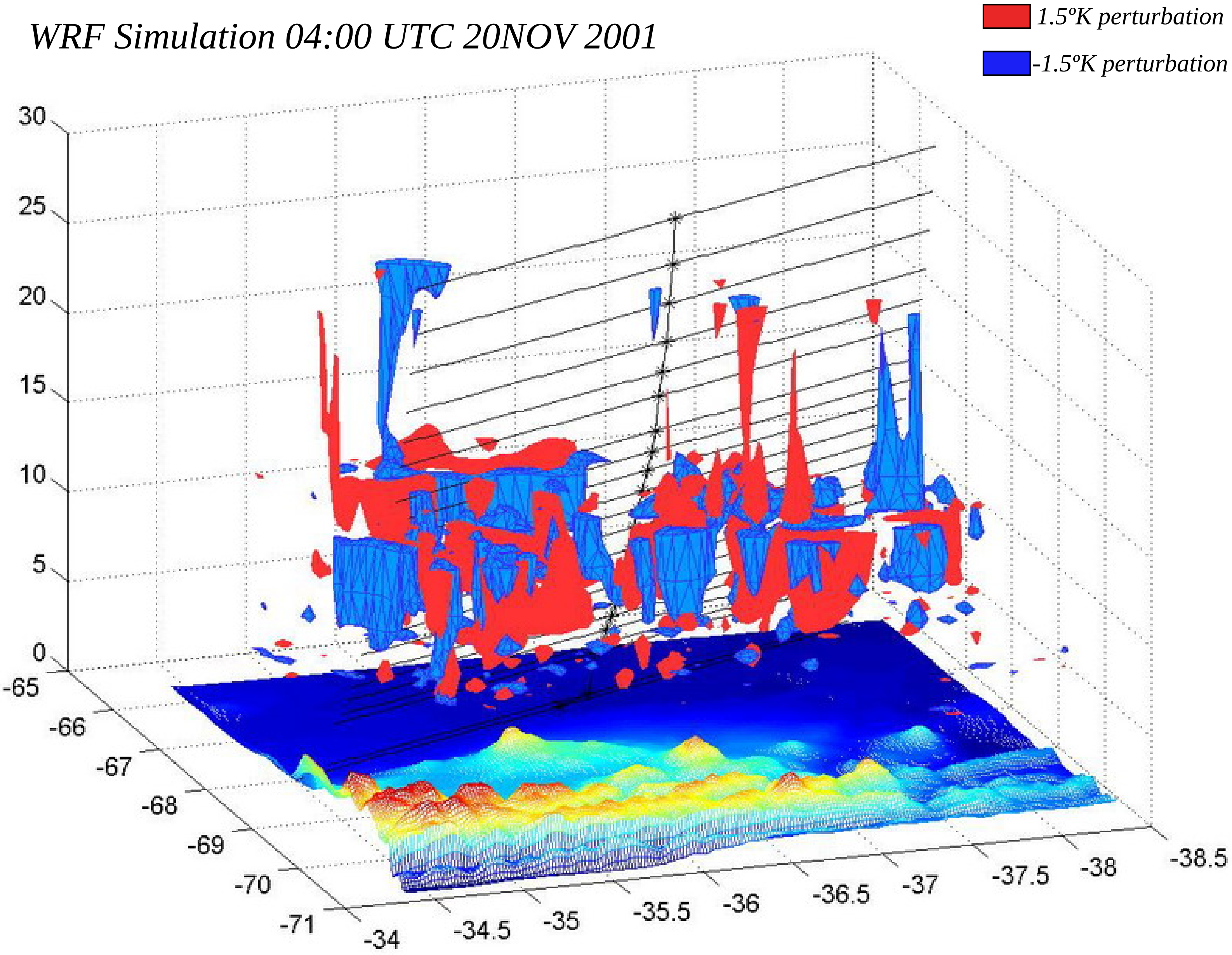

WRF Simulation 04:00 UTC 20NOV 2001
1.5ºK perturbation
-1.5ºK perturbation
30
25
20
15
10
5
0
-65
-66
-67
-68
-69
-70
-71
-34
-34.5
-35
-35.5
-36
-36.5
-37
-37.5
-38
-38.5

WRF Simulation 04:00 UTC 20NOV 2001

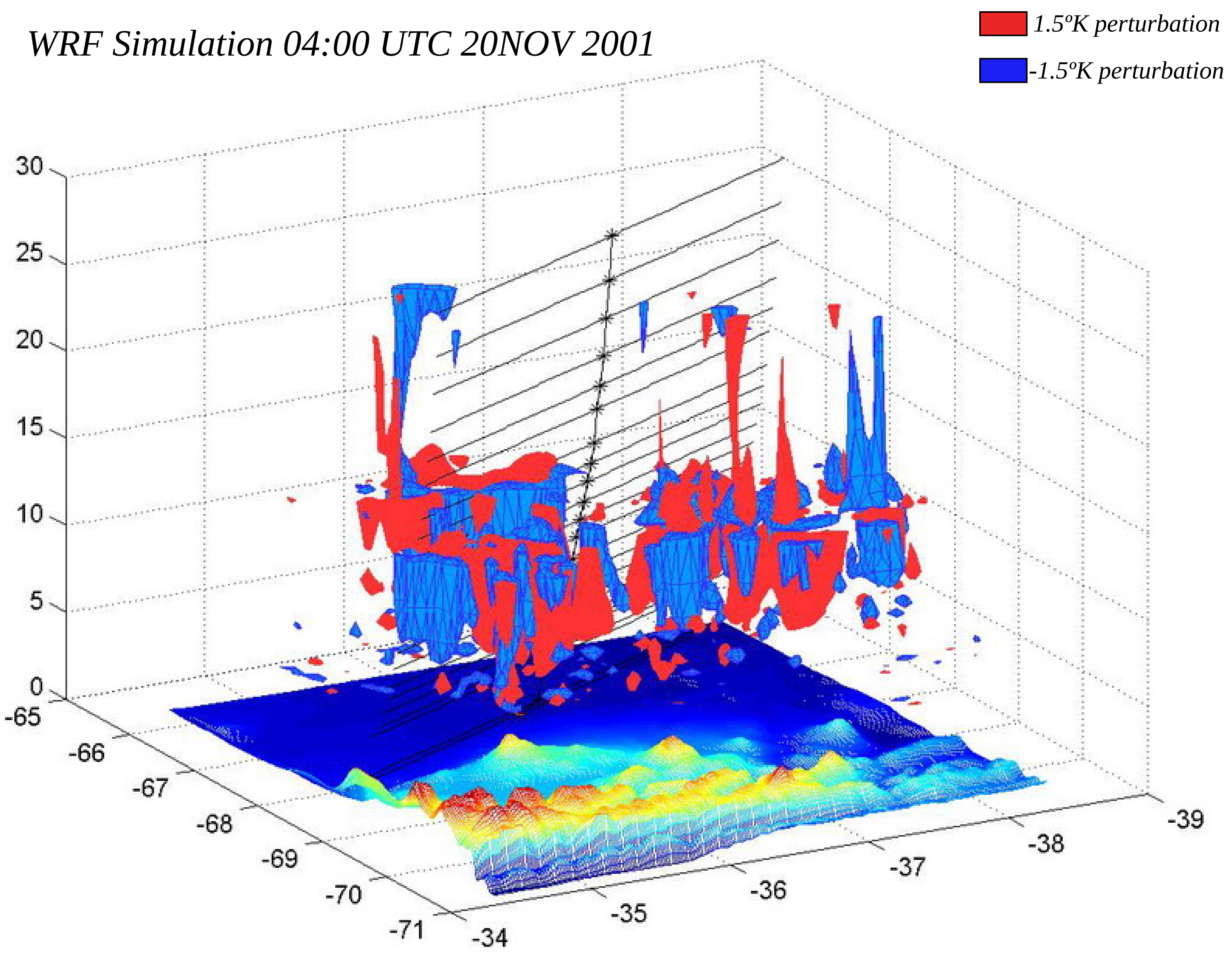

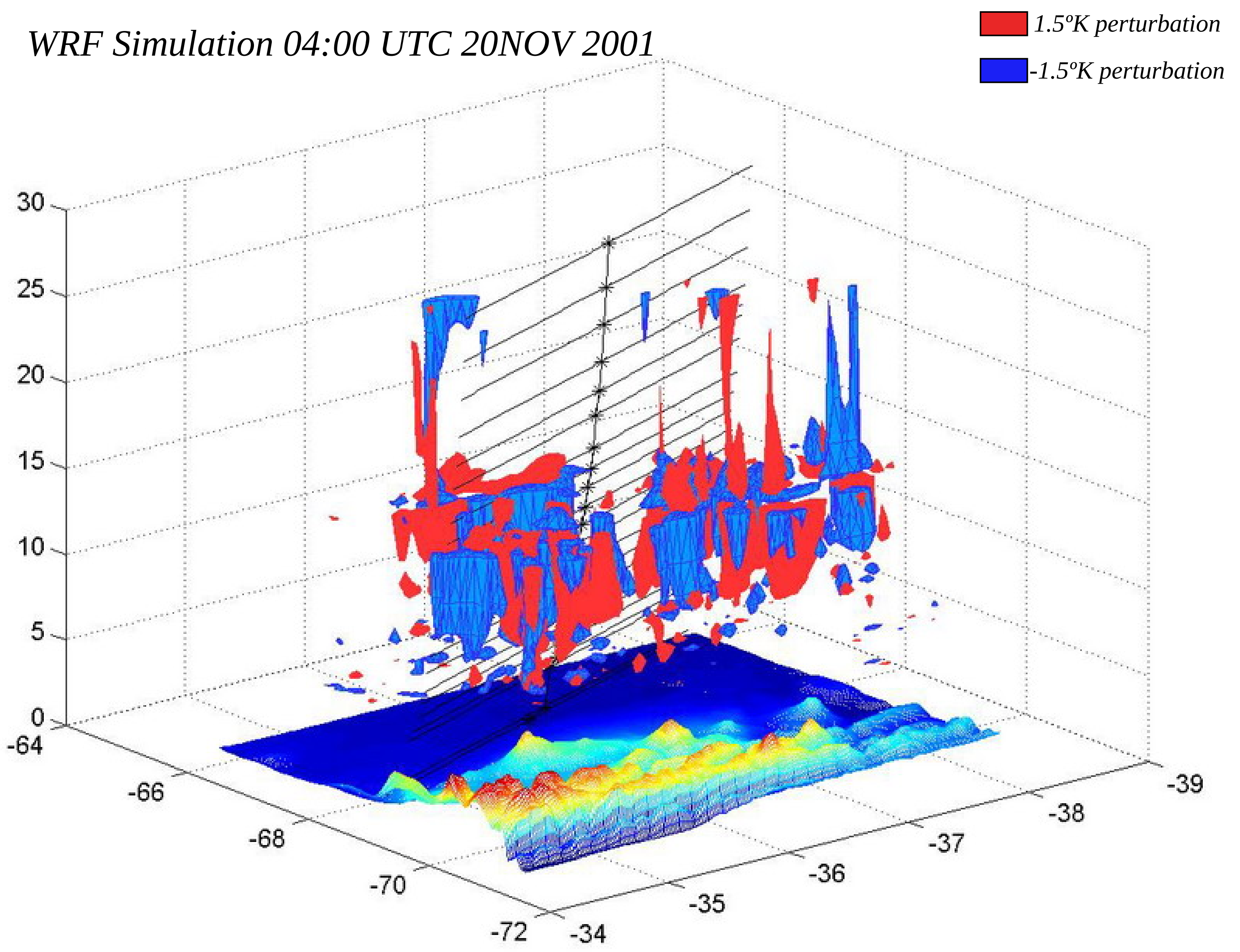
WRF Simulation 04:00 UTC 20NOV 2001
1.5ºK perturbation
-1.5ºK perturbation
30
25
20
15
10
5
0
-64
-66
-68
-70
-72
-34
-35
-36
-37
-38
-39

WRF Simulation 04:00 UTC 20NOV 2001

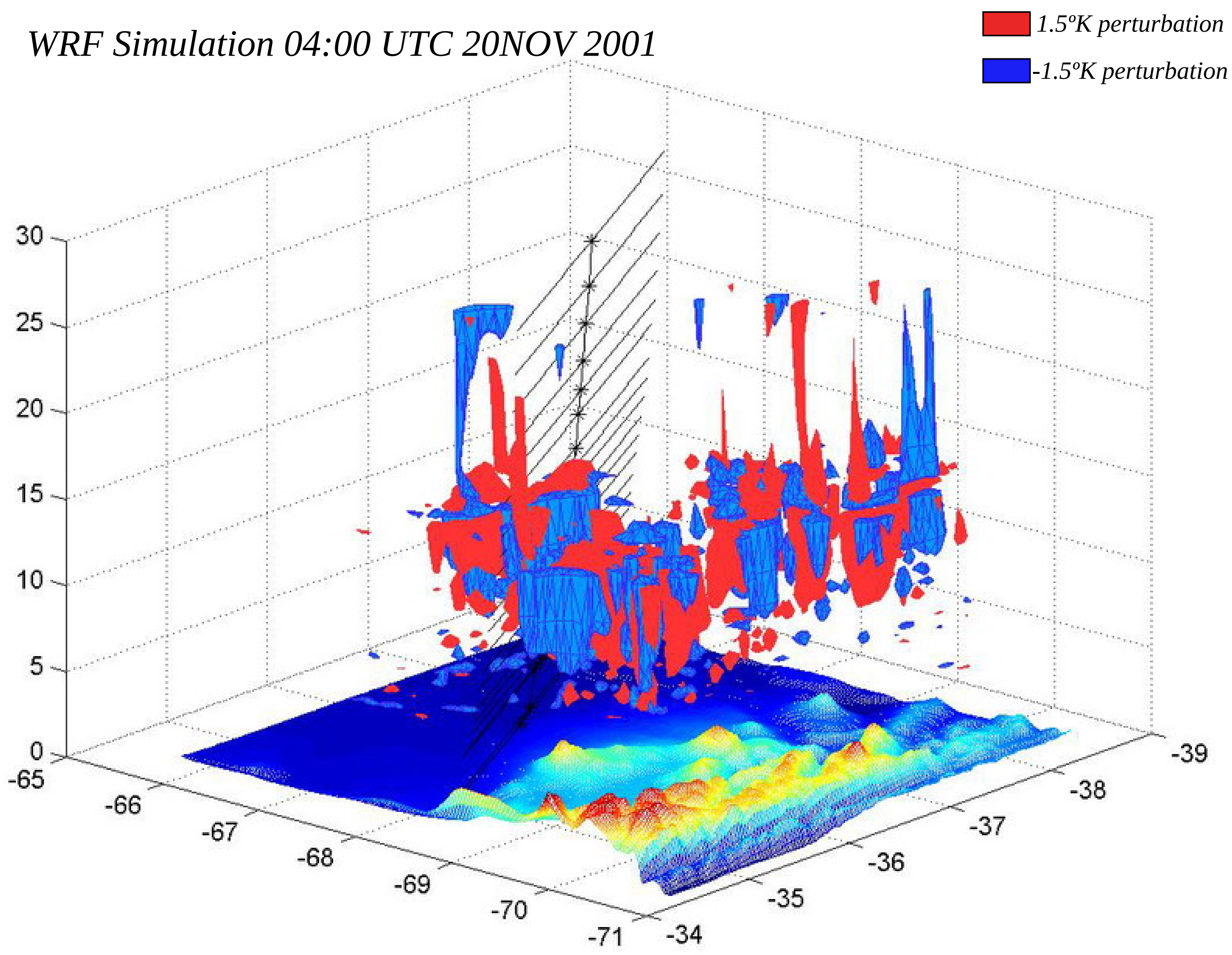

WRF Simulation 04:00 UTC 20NOV 2001

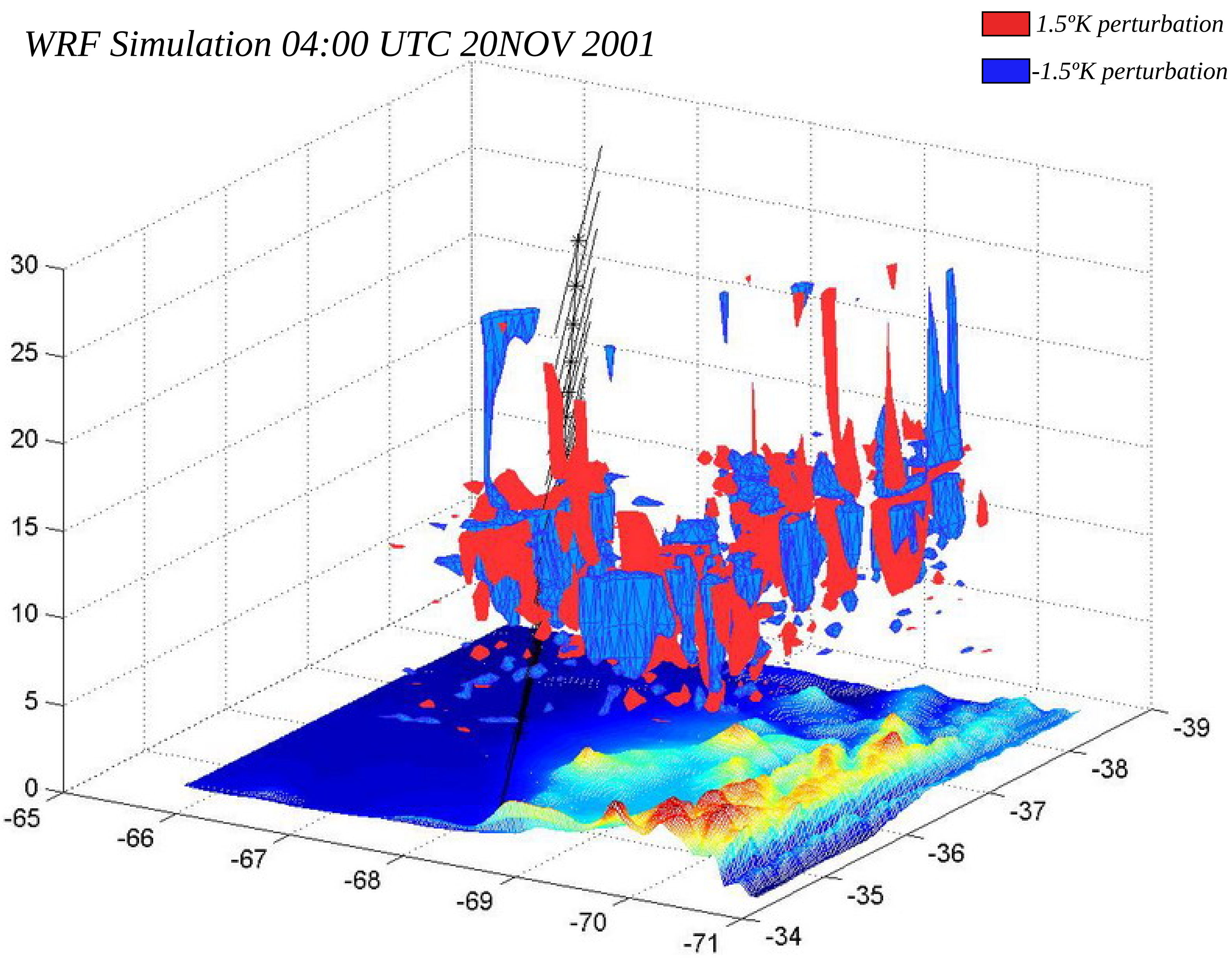

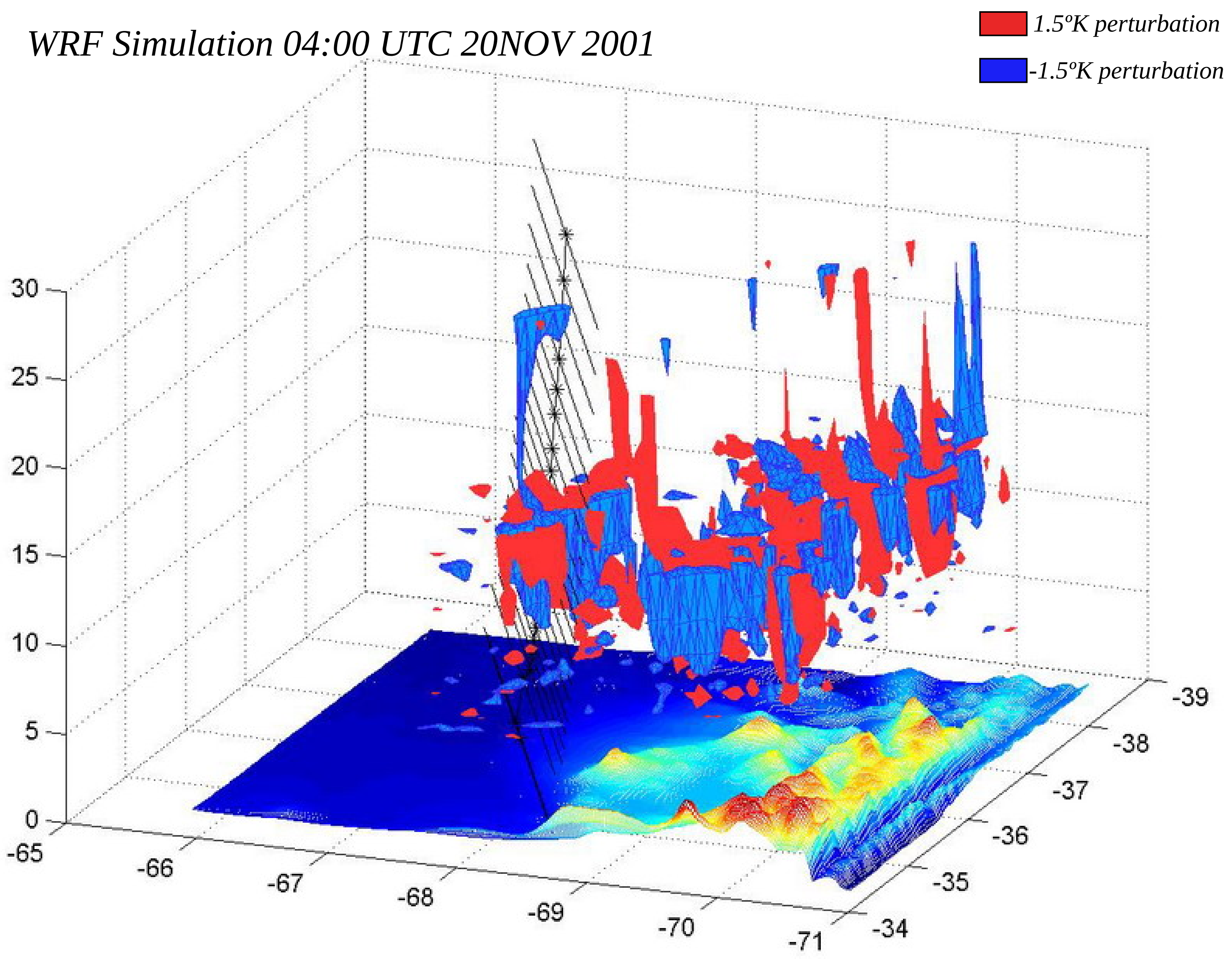
WRF Simulation 04:00 UTC 20NOV 2001
1.5ºK perturbation
-1.5ºK perturbation
30
25
20
15
10
5
0
-65
-66
-67
-68
-69
-70
-71
-34
-35
-36
-37
-38
-39

WRF Simulation 04:00 UTC 20NOV 2001

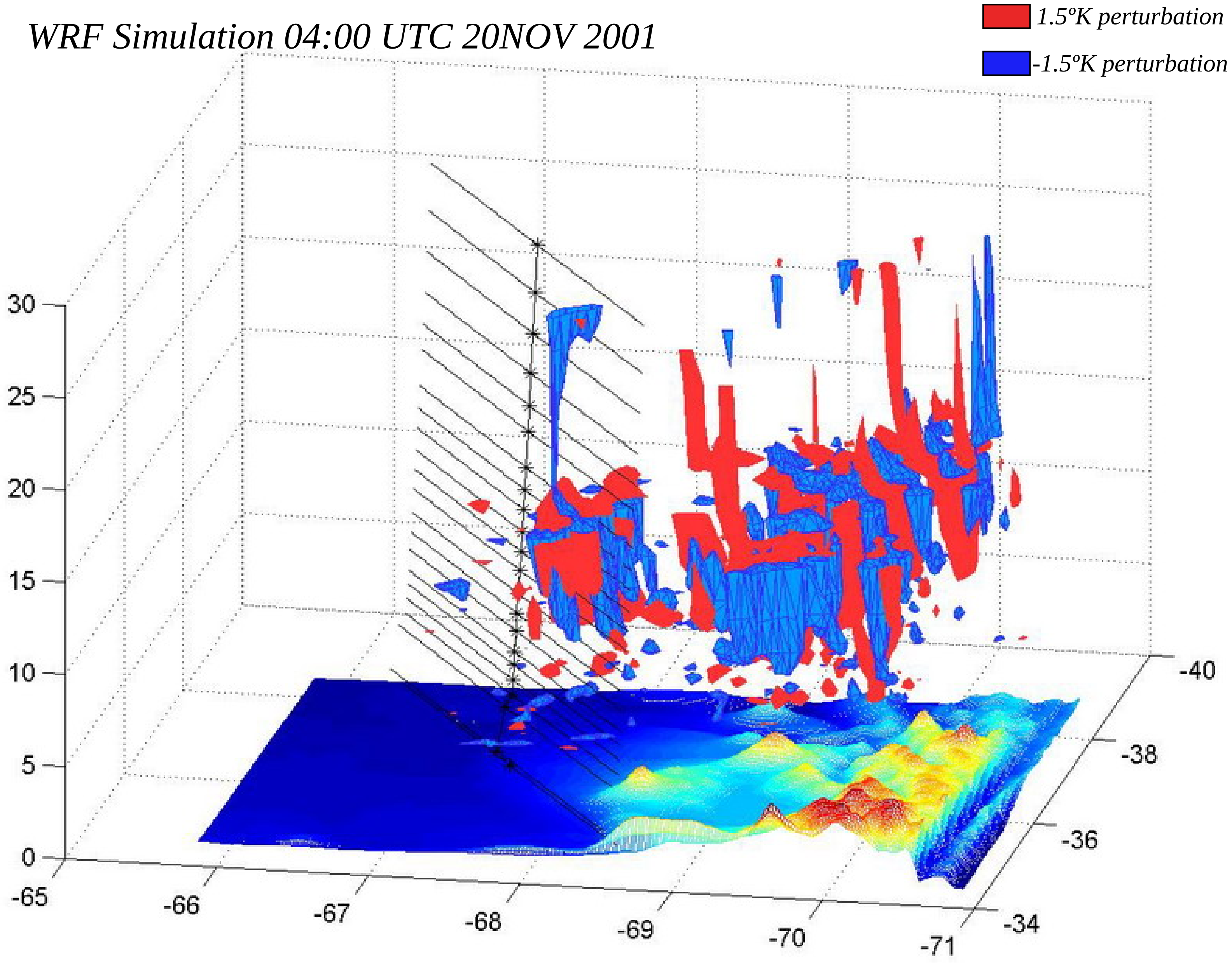

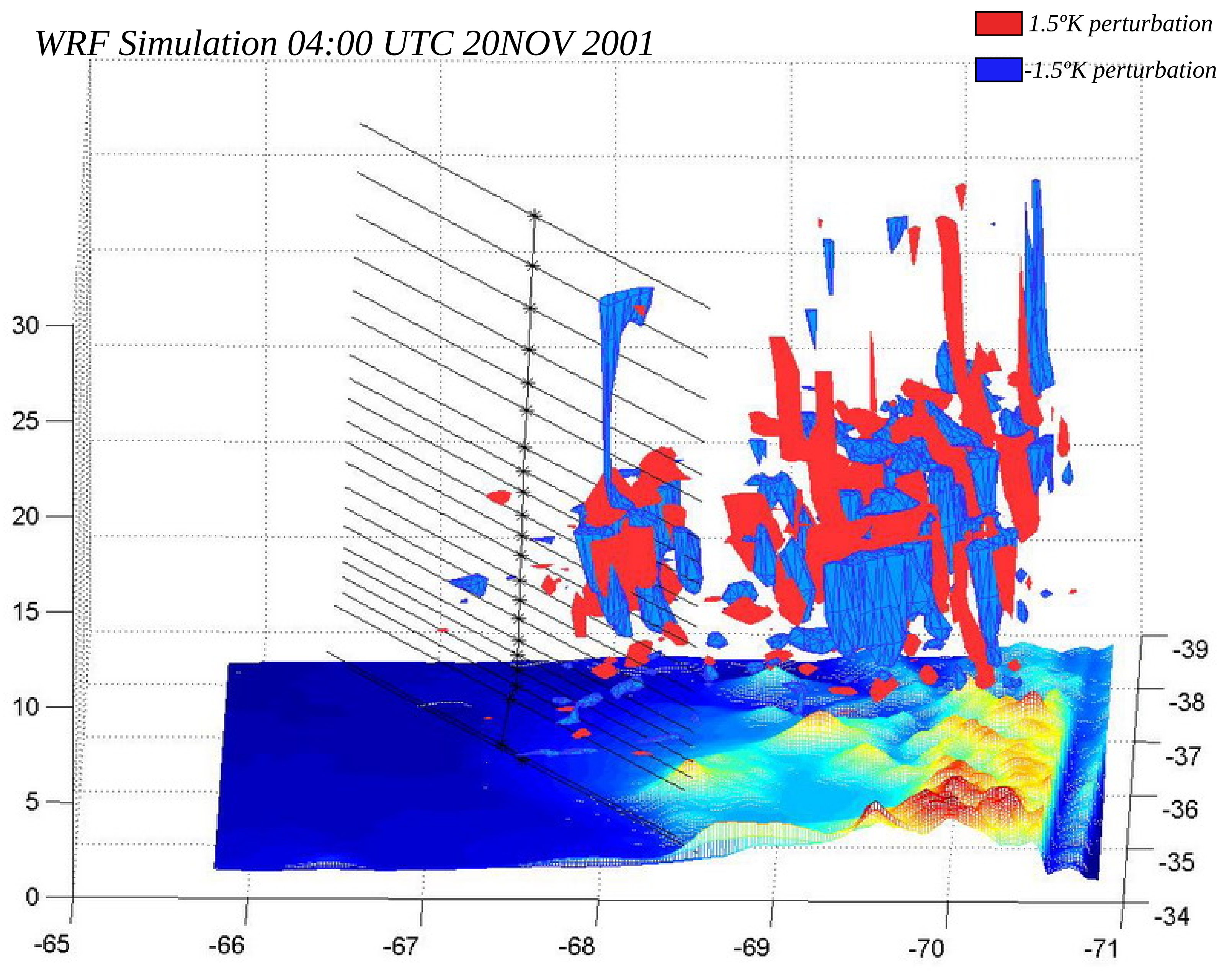
WRF Simulation 04:00 UTC 20NOV 2001
1.5ºK perturbation
-1.5ºK perturbation
30
25
20
15
10
5
0
-65
-66
-67
-68
-69
-70
-71
-39
-38
-37
-36
-35
-34

WRF Simulation 04:00 UTC 20NOV 2001

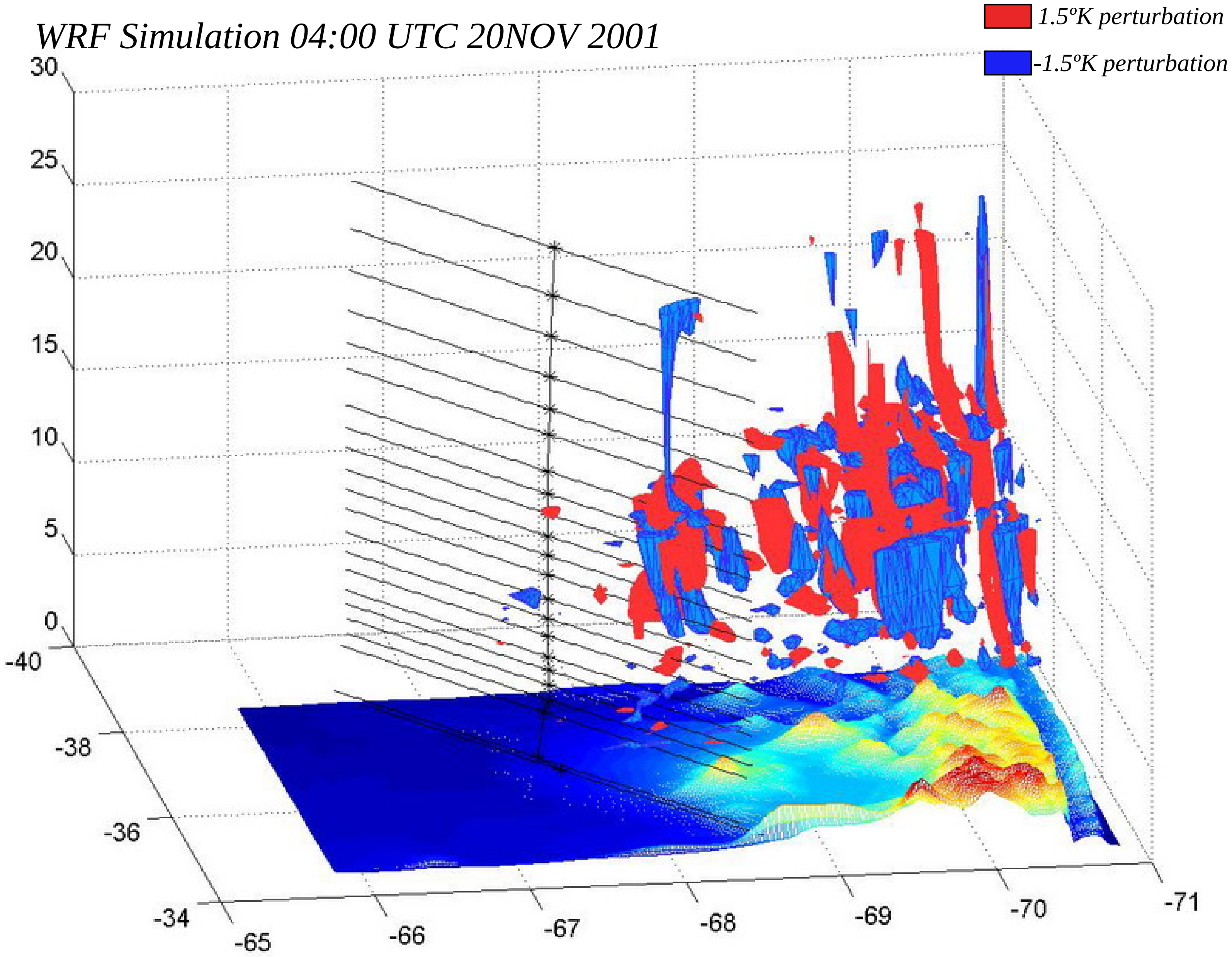

WRF Simulation 04:00 UTC 20NOV 2001

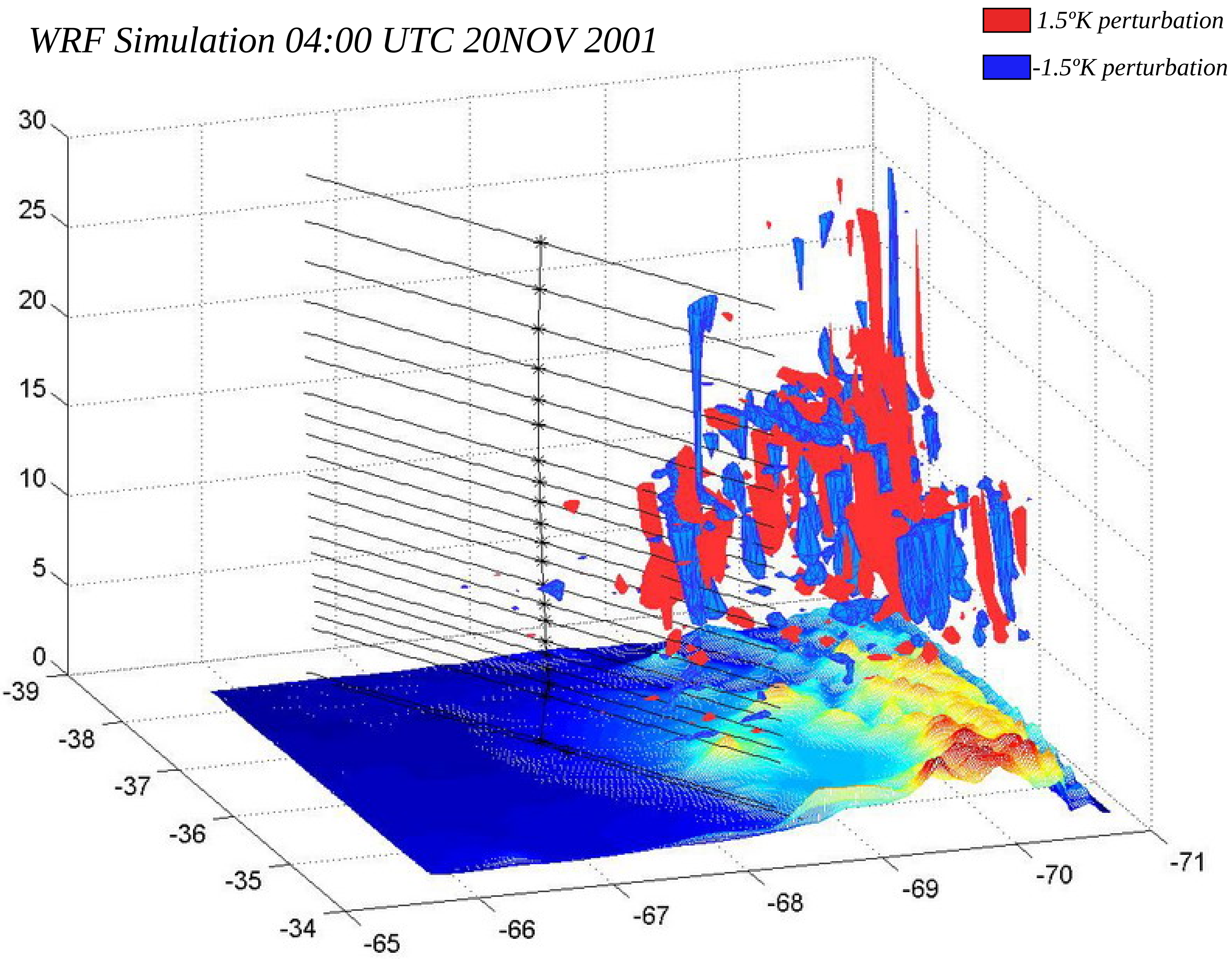

WRF Simulation 04:00 UTC 20NOV 2001

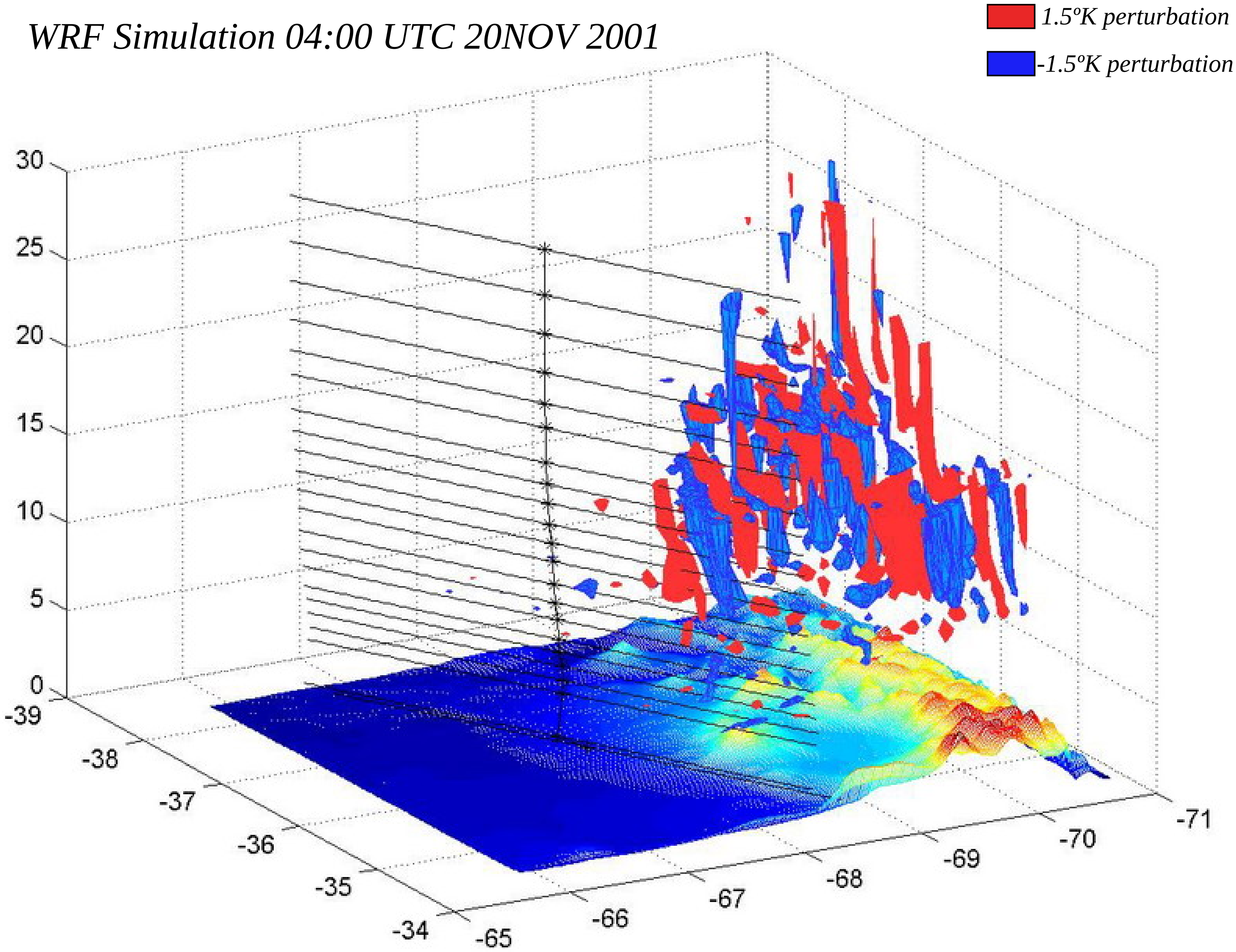

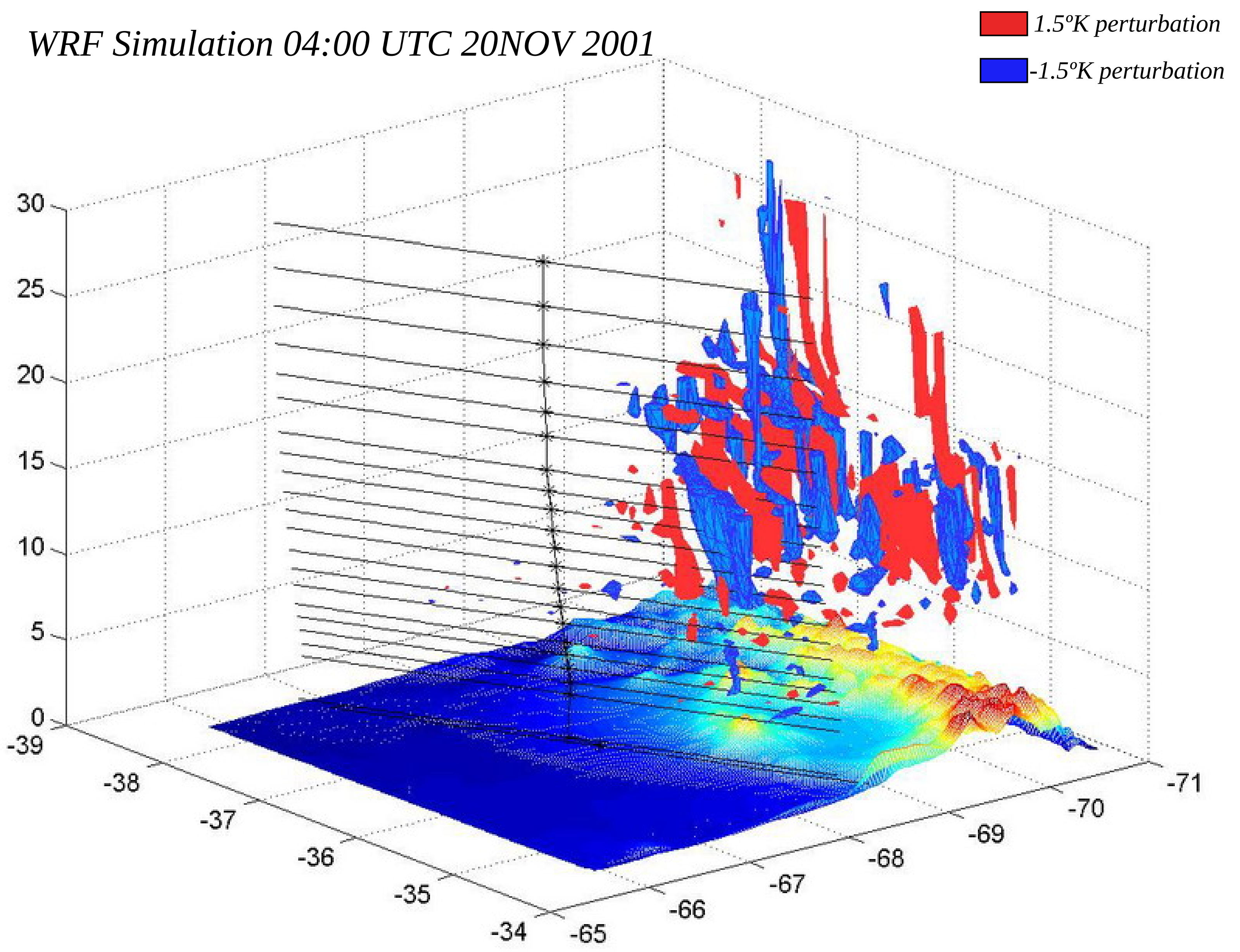

WRF Simulation 04:00 UTC 20NOV 2001
1.5ºK perturbation
-1.5ºK perturbation
30
25
20
15
10
5
0
-39
-38
-37
-36
-35
-34
-65
-66
-67
-68
-69
-70
-71

WRF Simulation 04:00 UTC 20NOV 2001

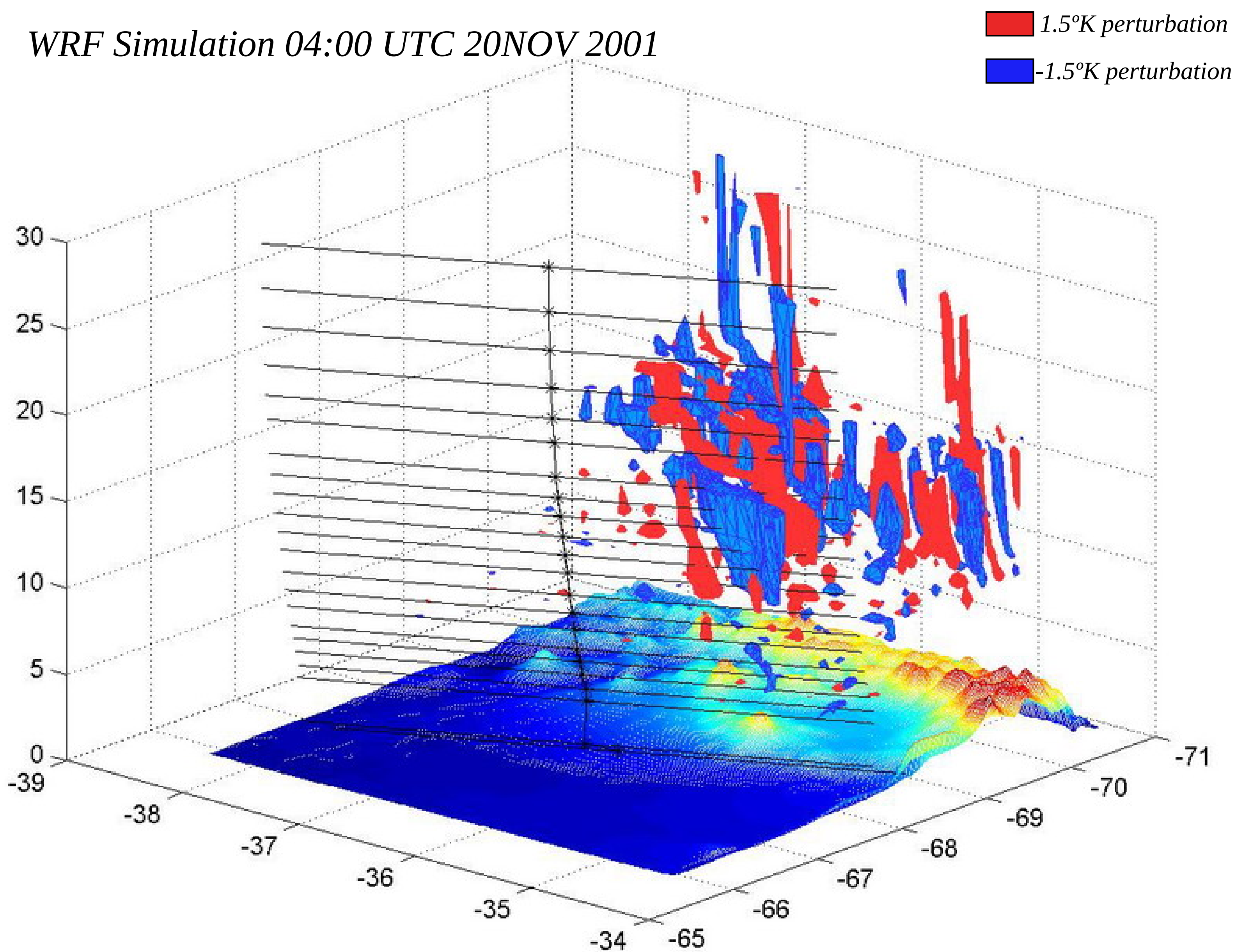

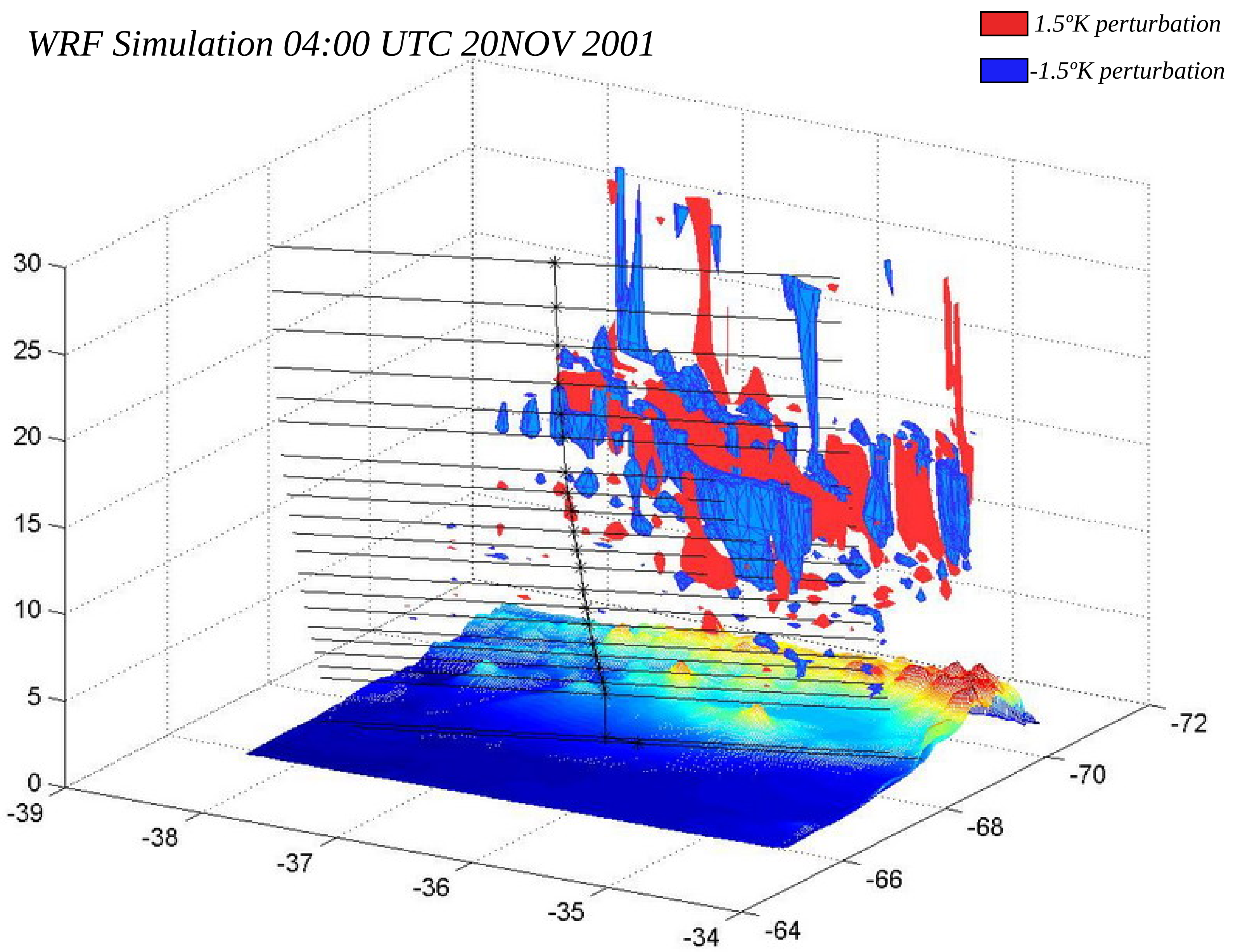
WRF Simulation 04:00 UTC 20NOV 2001
1.5ºK perturbation
-1.5ºK perturbation
30
25
20
15
10
5
0
-39
-38
-37
-36
-35
-34
-64
-66
-68
-70
-72

Comments:

- *In spite of the unquestionable progress achieved in the understanding of atmospheric oscillations from RO observations, background refraction and expected distortions imposed by the relative geometry of wave phase surfaces, lines of sight and of tangent points during each occultation restrict, to a certain extent, the quantitative significance of GW climatologies.*

- *Global observations allow to quickly detect events of interest and get insight into specific regions or time intervals of interest. These must be complemented by mesoscale simulations.*

Thank you !!